HOLLOW MICROSHELL THROUGH LAYER-BY-LAYER SELF-ASSEMBLY OF CHITOSAN/ALGINATE ON *E. COLI*

Michael Yilma Yitayew

Biomat'X Laboratories

Department of Biomedical Engineering

Biological and Biomedical Engineering Program

McGill University, Montreal

A Thesis Submitted to McGill University in Partial Fulfillment of the Requirements of

The Degree of Master of Engineering (M. Eng)

December 2019

TABLE OF CONTENTS

ABSTRACT (ENGLISH)

Hollow microspheres prepared via layer-by-layer (LbL) self-assembled polymers have become a growing interest for developing biocompatible delivery systems for drugs, imaging probes and other macromolecules. The development of these capsules benefits from ease of fabrication, versatility of materials being used and its ability to be tuned to the application by incorporating pH-sensitivity as well as targeting molecules. The LbL method has been used to construct capsules for delivering anti-cancer drugs, insulin and other therapeutics. Furthermore, previous work done in the lab has exploited this technique to obtain polyelectrolyte-coated *E. coli* for use as a bio-recognition element and discovered that a hollow polyelectrolyte capsule can be formed by spontaneous cell lysis. Following that observation, the current project aims to develop a protocol for making hollow capsules by LbL assembly of natural polyelectrolytes onto *E. coli,* subsequently lysing the cells and evaluating their efficacy using quantum dots as cargo. The study found that four bilayers of chitosan/alginate can be produced on the surface of the *E. coli* cells with good stability/minimal aggregation as verified by zeta-potential measurements. TEM and confocal microscopy were also used to characterize the capsule formation, thickness and morphology. Cell lysis was performed using 1% Triton-X buffer with EDTA and lysozyme, which resulted in empty vesicles with a wall thickness of ~50 nm and similar dimensions as the cell template. The design of a tunable and biocompatible delivery system is crucial in controlling the biodistribution of imaging probes to enhance efficacy in the targeted site as well as lower toxicity.

ABSTRACT (FRENCH)

Les microsphères creuses formées par auto-assemblage couche par couche (LBL) de polymère présentent un intérêt grandissant pour le développement de système biocompatibles de délivrance de médicaments, de sonde d'imagerie ainsi que d'autres types de macromolécules. Le développement de ces capsules bénéficie de procédés de fabrication simples, d'une large variété de matériaux disponibles, ainsi que d'une bonne adaptabilité à leurs applications par l'incorporation une sensibilité au pH et des molécules pour le ciblage. La méthode LBL a été employée pour construire des capsules pour la délivrance de médicaments anticancéreux, d'insuline et d'autres thérapies. De plus, les travaux antérieurs du laboratoire ont utilisé cette technique pour obtenir une bactérie *E Coli* revêtue de polyélectrolyte utilisée comme élément de bioreconnaissance et ont abouti à l'obtention d'une capsule creuse de polyélectrolyte par lyse cellulaire spontanée. Suite de ces observations, le projet actuel vise à développer un protocole pour la fabrication de capsules creuses par assemblage LBL de polyélectrolytes naturels sur *E coli* et lyse cellulaire ainsi que l'évaluation de leurs capacités par encapsulation de points quantiques. L'étude démontre que 4 bicouches de chitosan / alginate peuvent être assemblés à la surface de *E. Coli* et présentant une bonne stabilité comme le confirme les mesures de potentiel zeta. Les microscopies TEM et confocales ont aussi été employées pour caractériser la formation des capsules, leur épaisseur et leur morphologie. La lyse cellulaire a été effectuée en employant un tampon 1% Triton-X contenant de l'EDTA et du lisozyme, résultant en la formation de vésicules vides de 50 nm d'épaisseur et des dimensions similaires à la cellule modèle. La conception d'un système de délivrance sur mesure et biocompatible est crucial dans le contrôle de la biodistribution de sondes d'imagerie pour améliorer l'efficacité de ciblage et diminuer la toxicité.

ACKNOWLEDGEMENT

I would like to thank my supervisor Prof. Maryam Tabrizian for her support, advice and guidance throughout this project. Working with her has been an invaluable learning experience and I am extremely grateful to have had such an opportunity. I would also like to thank my labmates at Biomat'X laboratories for all their help and support throughout this endeavor. Specifically, I would like to thank Brandon Paylis for answering my questions regarding *E. coli* culture and spectrophotometry measurements; Saadia Shoaib, who helped me with fluorescence microscopy; Rafael Castiello for answering my questions regarding layer-by-layer assembly; and Kaushar Jahan for her expertise on everything chitosan related. I also extend my gratitude to the rest of our current lab members as well as ex-lab members for their support and friendship.

I would also like to thank Ms. Jeannie Mui at the Facility for Electron Microscopy Research for training and guidance related to the use of TEM, and Dr. Nelly Vuillemin at the Advanced Bioimaging Facility for the training on confocal microscopy.

Additionally, I would like to thank my family for their continuous and unconditional love and support throughout my entire academic journey. My mom and dad have always believed in me and pushed me hard so I can achieve my best. Their encouragement and dedication are the reasons I am where I am today. I would also like to extend my gratitude to my younger brother. I can always rely on him to call and voice my frustrations. I would also like to express gratitude to my friends for believing in me, and especially to my fellow graduate student friends, who share the same road and have stuck with me through the ups and downs of grad school. I truly appreciate you all.

LIST OF FIGURES

LIST OF FORMULAS

Beer-Lambert equation

$$A = log_{10}\frac{I_o}{I}$$

A→absorbance I_o→incident light intensity I→transmitted light intensity

Sauberey equation

$$\Delta f = -\frac{2{f_o}^2}{A(\mu_q\rho_q)^{1/2}}\Delta m$$

Δf→frequency change f_o→resonance frequency Δm→mass change ρ_q →density of quartz

A→piezoelectrically active surface area of quartz μ_q→shear modulus of quartz

Henry equation

$$\mu_E = \left(\frac{2\varepsilon\zeta}{3\eta}\right)f(\kappa r)$$

μ_E→ electrophoretic mobility ε→dielectric constant η→absolute zero-shear viscosity of medium

ζ→zeta potential $f(\kappa r)$→Henry function, κr measures the ratio of particle radius/ Debye length

Henderson-Hasselbalch equation

$$pH = pK_a + log_{10}\frac{[A^-]}{[HA]}$$

pH→ pH of the buffer solution pK_a→acid dissociation constant of the buffer

$[A^-]$→ concentration of conjugate base $[HA]$→ concentration of acid component of buffer

PREFACE

This thesis contains original, independent research completed by the author, Michael Yilma Yitayew under the direct supervision of Prof. Maryam Tabrizian. All experiments, figures and data analysis were completed by the author. The abstract was translated to French by Dr. Hugo Salmon.

1. INTRODUCTION

1.1 Rationale

The synthesis of hollow microcapsules has been of great interest in the development of new delivery systems due to their function to encapsulate and mediate controlled release of a wide-variety of drugs, nanoparticles and other macromolecules. Their use became prominent due to their ability to incorporate polar molecules and prove to be a more stable system with better permeability than liposomes.[1] The most established method to fabricate such capsules uses calcium carbonate ($CaCO_3$) microspheres or other salt particles as a building block or template for polymer encapsulation and hollow capsules are formed by removing the template using a chelating agent such as ethylenediaminetetraacetic acid (EDTA).[2,3] In recent years, researchers have further expanded towards the use of biological templates such as bacteria as well as eukaryotic cells to fabricate hollow capsules with varying shapes and sizes. Using biological templates presents a potential for the development of an easier, more efficient and biocompatible protocol for the fabrication of these capsules.[1]

The encapsulation of the template occurs as a result of electrostatic interactions between oppositely charged polyelectrolytes in a process called layer-by-layer self-assembly (LbL), which form a highly organized nano-shell around the template.[4] The application of LbL was initially limited to planar surfaces but has recently expanded to colloidal and other complex 3D surfaces. Some notable examples including coating of nanoparticles for controlled release of cancer drugs[5] and formation of polyelectrolyte capsules on red blood cells for immunocamouflage.[6]

Furthermore, the Biomat'X laboratory has previously exploited this technique to obtain chitosan/DNA-coated *E. coli* for use as a bio-recognition element in DNA hybridization and discovered that a hollow shell was formed by spontaneous cell lysis.[7] The proposed thesis aims to explore this phenomenon further and develop a stable hollow microcapsule by cell lysis after LbL assembly of chitosan/alginate onto *E. coli.* The study will incorporate quantum dots into the microcapsule to show proof-of-concept and study capsule properties as a controlled release carrier. The process is illustrated below in Figure 1.1.

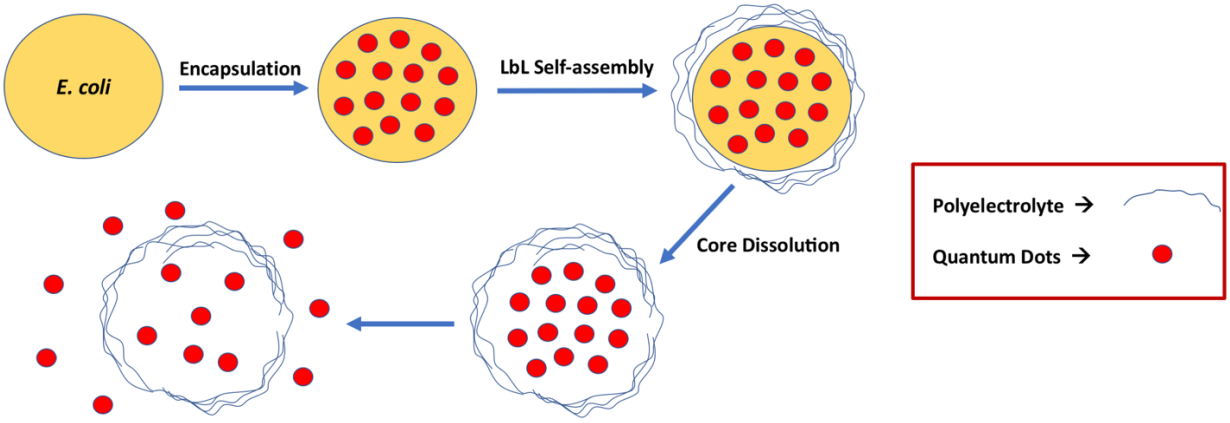

Figure 4.1: Schematics representing the proposed hypothesis of this study. Quantum dots will be incorporated into the *E. coli* before the construct is encapsulated with polyelectrolytes (Chitosan/Alginate). The cell will be subsequently removed to yield a hollow microcapsule containing quantum dots.

The proposed study aims to develop a protocol that is unprecedented due to its ability to incorporate sensitive biological polymers to create monodisperse capsules with a variety of shapes and sizes using cells as template. Furthermore, it also uses mild conditions for the dissolution of the core template (*E. coli*). The protocol used for core dissolution can be adjusted for the microshell

to retain and encapsulate materials in the cell template such as plasmid DNA or imaging probes, which can be inserted into the bacteria before polymer encapsulation as shown in Figure 1.1. Additionally, using chitosan/alginate as capsule material improves the biocompatibility of the system by reducing immunogenicity *in vivo* and slow degradation of the material via enzymes in the body. This eliminates long term toxicity effects that are seen with non-degrading polymers used for capsule fabrication.[3]

1.2 Hypothesis and Objectives

The goal of this project is to develop hollow microcapsules using chitosan and alginate as natural polyelectrolytes. A layer-by-layer self-assembly technique is used for the formation of such capsules and *E. coli* DH5α cells is used as a sacrificial template. Once this template is successfully removed, the feasibility of this hollow construct is tested using quantum dots as a cargo for these hollow capsules. It is hypothesized that lysis of coated *E. coli* produces a hollow stable microshell that can be used for drug/fluorescent imaging probe delivery. The objectives of this study are as follows.

1. **Encapsulation of *E. coli* DH5α cells with alternating layers of chitosan and alginate.**

   Encapsulation of live cells and characterization of layer thickness, morphology, size and distribution of coated particles as well as surface charge using appropriate analytical tools including confocal and transmission electron microscopy as well as zeta-potential analysis. It also includes investigation and optimization of factors that influence the formation of such bilayers like pH, ionic strength, buffer composition using polystyrene microspheres and fixed *E. coli* cells as a proof-of-concept templates.

2. **Determination of a suitable cell lysis protocol to form hollow microspheres.**

   Determination of a suitable lysis protocol by testing procedures that are well-established in the literature for the lysis of *E. coli*, which include detergent-based buffers, alcohols and other reagents. It also includes characterization of the resulting vesicles using TEM and live/dead assay for viability of the cell template as well as the size and morphology of the hollow vesicles.

3. **Encapsulation of quantum dots into cells before LbL coating as a cargo for the subsequent hollow vesicles.**

   Examination of the hollow vesicles as a proof-of-concept for a delivery system by utilizing quantum dots as cargo and studying the viability and stability of the system using confocal microscopy and TEM.

2. LITERATURE REVIEW

2.1 Nano-sized delivery systems for therapeutics

Delivery systems play essential roles in mediating how drugs, imaging probes and other therapeutic agents circulate and affect the body. These systems allow for the controlled release of substances, targeted delivery to specific areas of the body, and limited adverse immune reactions that would otherwise interfere with the goal of the therapeutics.[8,9] As a result, the effective dose of therapeutic substances can be lowered and this can help limit toxicity issues that can arise from administration of high doses in combating fast elimination of substances by the body.[5] Examples of these systems can be classified into 2D and 3D systems. 2D applications include modified implant surfaces, microneedles and skin patches whereas 3D applications include materials such as liposomes, micelles, nanoparticles and hollow polymer shells.[5,10]

Some of the critical characteristics to design such systems are the stability of the construct, its ability to encapsulate its cargo, and mediate release of the material. There has been an increasing need for the design of controllable smart delivery systems instead of passive delivery systems as they are more responsive and present higher specificity.[11,12] This can include materials that can respond to environmental stimulus such as pH, temperature, ionic strength, redox states or enzymatic reactions. This versatility also controls their mode of delivery as illustrated in Figure 2.1, where different internalization pathways expose the material to different environments.[8,13] Hollow microcapsules are an interesting material in this regard due to increased loading capacity and better permeability to a wide variety of substances.[14]

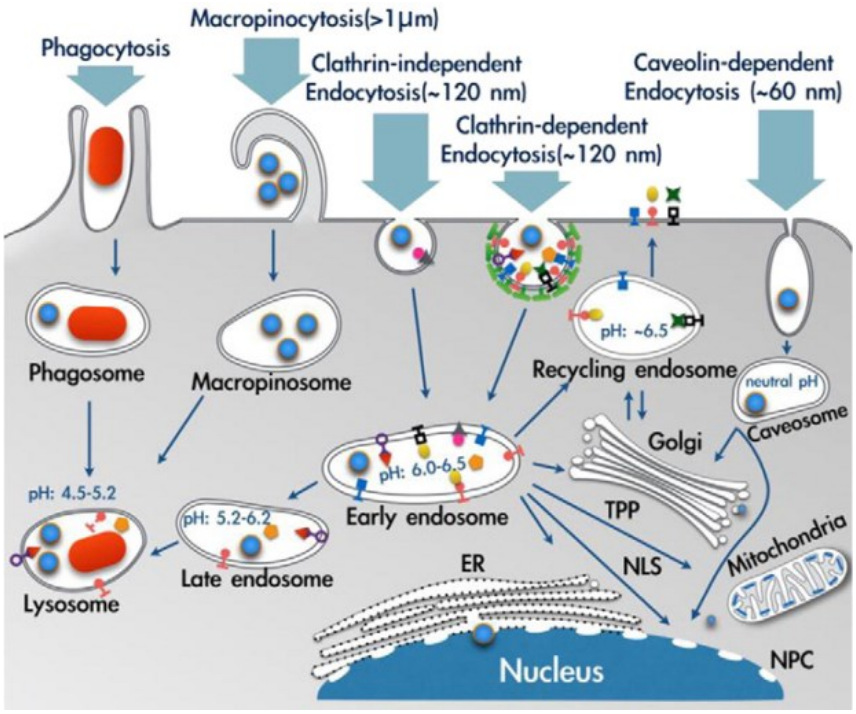

Figure 5.1: Illustration of the fate of nano-constructs during uptake by cells in the body. The different methods of endocytosis including passive and active as well as size-based exclusion are demonstrated. Image reproduced from ref [11], Copyright 2014 with permission from Elsevier.

2.2 Hollow capsules

Hollow capsules are favored as delivery systems due to facile synthesis method and ability to control the release of core material by manipulating the number and composition of the capsule material.[15] They also allow for a bigger volume of cargo to be stored inside. Furthermore, they are an improved alternative to liposomes due to their ability to encapsulate polar substances. Current methods to synthesize hollow capsules include templating, emulsification and layer-by-layer self-assembly.[16] Templating involves the building of capsule wall around a solid spherical template via solute deposition or surface reactions onto the template. Once this is done, the template is removed to leave the hollow capsule behind. Layer-by-layer assembly follows a similar protocol but

exhibits fine control over layer composition due to the ability to manipulate the number of polymer layers as well as the thickness through changes in pH and ionic strength. Lastly, emulsification utilizes oil droplets as a template material, which then determine the size and shape of the microcapsule.[16,17]

From the aforementioned protocols for hollow capsule synthesis, LbL method is favoured due to increased control of permeability as well as the ability to design smart and responsive capsules. Capsule size, permeability and release profile can all be mediated by manipulating its environment and this makes it appealing for on-demand delivery at the active size of the therapeutics.[18] Furthermore, LbL capsules can exhibit selective permeability towards outside factors allowing them to shield the cargo from unwanted degradation and other side effects.[19]

2.3 Development of self-assembled thin-films

The use of self-assembled nanolayers to control material surface properties such as surface wettability, permeability and biocompatibility is a well-established phenomenon for enhancement of material performance. In the context of capsule formation, this influences the capsule interaction with the body and its ability to release cargo in a timely fashion.[10,20] Control over surface properties is especially important in the development of biomaterials to protect from degradation or elimination in the body as well as retain viability and functionality. Self-assembly of these nanofilms can be done with nanometric precision and be applied to both macroscopic biomaterials such as bone implants and stents as well as micro and nano-biomaterials such as microneedles, cell encapsulations, liposomes and nanoparticles.[17] This concept can be used to reduce implant degradation, improve integration of biomaterial with the body, control release of therapeutics and

more. As a result, several techniques have been developed over the years for controlled synthesis of self-assembled thin films on a wide range of surface morphologies and geometry.

Since the 1930s, the development of self-assembled nanolayers was mainly performed using the well-established and sophisticated Langmuir-Blodgett (LB) technique, named after Dr. Katharine Blodgett and Dr. Irving Langmuir who discovered it while working at General Electric Co.[21–23] The LB technique exploits amphiphilic molecules, which can be arranged at air-water interfaces due to the presence of both polar and non-polar regions on the molecule, to create monolayers following solvent evaporation.[17,23] The LB technique allows for the synthesis of highly ordered and densely packed monolayers with precise control over thickness (Figure 2.2). It can also be used to form multilayers by determining if dominant interaction between the molecules is hydrophobic-hydrophobic, hydrophobic-hydrophilic, or hydrophilic-hydrophilic.[23] However, LB requires sophisticated instruments and is more laborious method for developing thin films, which can create problems for scale-ups. The challenge arises from the necessity to be able to dip the material and therefore makes it difficult to apply onto particles or other complex surfaces.[24]

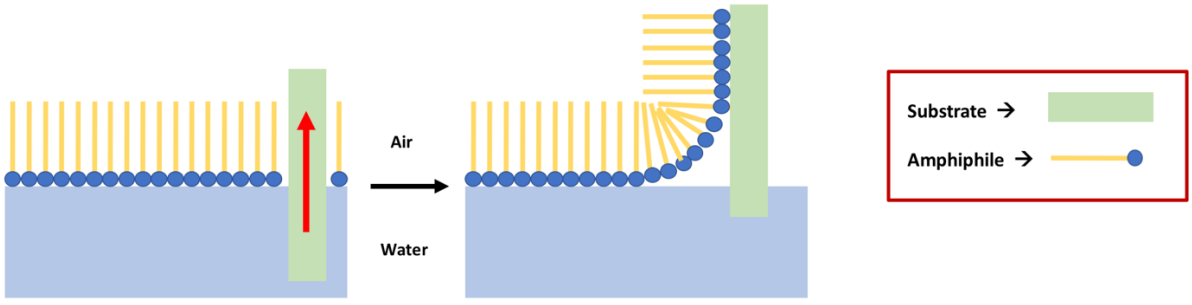

Figure 2.2: Schematic showing layer deposition via LB method.

In order to overcome some of the limitations of LB, a simpler technique was created by Dr. Jacob Sagiv in the 1980s, who used chemisorption of amphiphiles at the solid-fluid interface

to create what is now known as self-assembled monolayers (SAM).[25,26] Subsequent reactions can then be used to covalently link the monolayer to the surface in solution. The technique is now often used for modification of gold, silver, alumina and similar substrates.[27] The most commonly exploited chemistry for SAM is the use of layer molecules with terminal silane groups to bind free hydroxyl groups present on the material surface.[28]

2.4 Layer-by-layer self-assembly

Recently, layer-by-layer (LbL) self-assembly has emerged as a powerful tool to create thin films for material surface modification. The technique was first introduced by Iler [29] in the 60s when it was used to coat glass surfaces with colloidal particles but became increasingly popular in the early 90s with the work by Decher *et al*.[30,31], which made use of polyelectrolytes as layer materials instead.[17,20,32] This allowed for the expansion of the technique from its use on planar macroscopic surfaces to coating micro and nano-sized substrates with variety of shapes including colloids, liposomes and cells.[32] Generally, the formation of these films follows a repetitive process of polyelectrolyte adsorption, washing step, and adsorption of the oppositely charged polyelectrolyte (Figure 2.3). Electrostatic interactions between the oppositely charged polyelectrolytes are the established and main driving forces in the formation of these films[20], which allows for the creation of uniform layers that are not affected by the nature and topology of the substrate.[31] As a result, the technique produces robust, nanometer-thick layers using a variety of coating materials and core substrates with a multitude of applications ranging from material science to medicine.

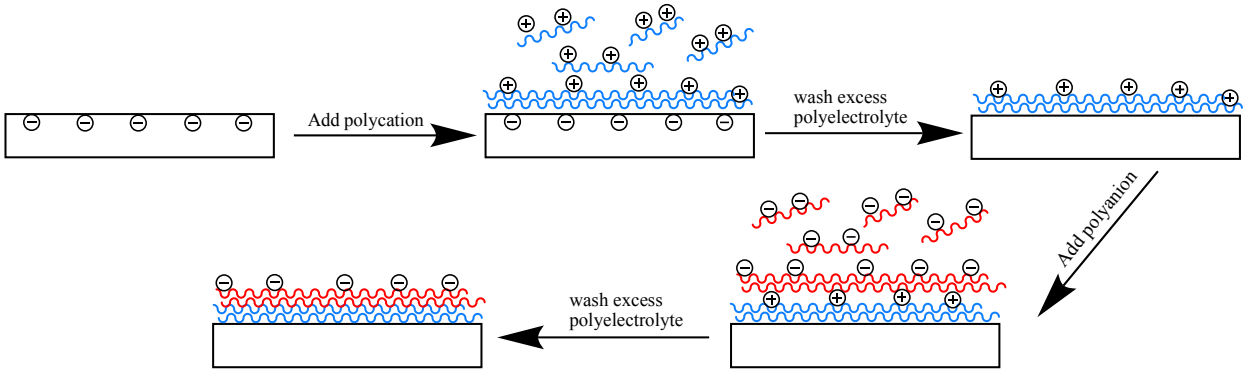

Figure 2.3: Schematic diagram showing the process of layer-by-layer self-assembly onto a negatively charged planar substrate.

The formation of complexes between oppositely charged polyelectrolytes occurs very fast and is driven by entropy due to the release of counter ions. Counter ions are present in aqueous solutions containing salt and they surround individual polyelectrolyte chains in solution. The formation of a layer complex between two oppositely charged polyelectrolytes results in the displacement of such ions from each polymer chain, and the speed at which this displacement occurs determines the speed of complex formation.[33] The entropic contribution of counterions is pronounced at low concentration and often described as the intrinsic charge compensation mechanism. On the other hand, high concentrations of counter ions diminish this effect and this phenomenon is described as the extrinsic charge compensation. In this scenario, the abundance of counterions inevitable force some of them to be trapped within the polyelectrolyte complex forming weakly adsorbed polyelectrolyte layers (Figure 2.4).[32]

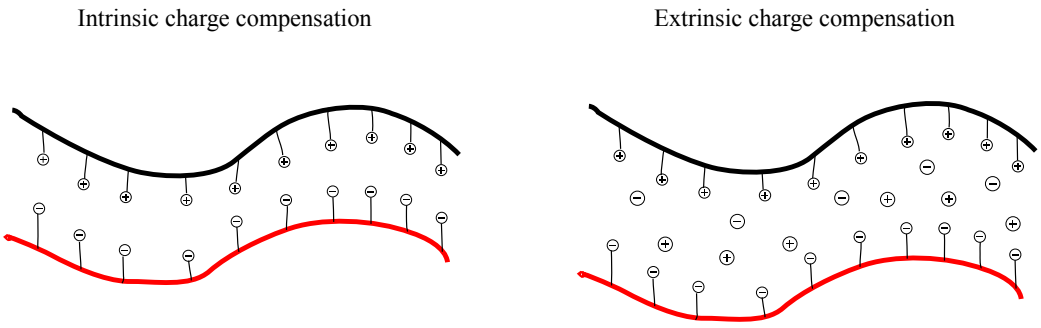

Figure 2.4: Schematic diagram outlining the mechanism for intrinsic and extrinsic charge compensation during polyelectrolyte complex formation.

Polyelectrolyte complex formation constant is seen to increase exponentially up to a chain length of six monomer units within the polyelectrolytes. Above this threshold, there are no significant differences seen on the complex formation constant with increasing monomer units. Furthermore, the consistency of these structures is controlled by the stoichiometric ratio of the two oppositely charged polymers. Two polyelectrolytes with a similar molar mass and appropriate ionic strength can form an organized "ladder-type" linear layer. On the other hand, drastic differences in molar mass can result in the longer polymer serving as a "host-molecule" and smaller chains can adsorb onto the longer polymer, with possible gaps in between them due to the presence of counterions.[34]

Compared with earlier methods of thin-film formation, LbL assembly provides versatility in terms of choice for layer material, solvent conditions and type of substrate, which makes it the preferred method for coating in biological applications where aqueous conditions are required.[20] This avoids issues with steric hinderance which can limit other coating techniques such as Langmuir-Blodgett (LB) and self-assembled monolayers (SAM). LB requires complex equipment and also restricts substrate size and film stability. On the other hand, SAM is restricted by the high

steric demand of covalent chemistry and the extreme lack of chemical reactions with 100% yield, which otherwise would affect functional group density.[31] Since its discovery, LbL assembly has been the preferred method for producing nanofilms over alternative methods such as SAM and LB due to large scale capabilities, versatility of substrate, precise control over structure of nanofilm, and mild fabrication conditions for improving material surface properties and/or biocompatibility.[20]

2.4.1 Materials

In recent years, materials used for LbL assembly have expanded with lipids, nanoparticles and other constituents incorporated in LbL constructs.[4,35] However, the most commonly used layer materials in LbL are polyelectrolytes, a class of polymers that are water soluble and contain dissociated ionic side groups that give the polymer chain a net charge. This property allows polyelectrolytes to adsorb onto charged substrates bearing the opposite surface charge. They are a very fascinating class of materials due to their dual characteristics of a highly charged electrolyte as well as macromolecular chain structure.[34] Examples of polyelectrolytes range from synthetic polymers such as poly(styrenesulfonate) and poly(allylamine hydrochloride) to natural polymers like proteins, DNA and synthetic-natural polymers such as chitosan and alginate. The properties of LbL capsules formed by each of these polymers are dependent upon the environment they are in and include factors like pH and ion concentration as well as biodegradability.[12,36] This is also correlated with the chemistry present in the polymer backbone as well as the dissociation constants of its side chain. For instance, polymer backbones that contain ester or amide bonds are more likely to be cleaved by enzymes in the body over aliphatic chains with linear carbon-carbon bonds.[37]

Polyelectrolytes are generally classified into strong and weak polyelectrolytes and the pKa of their side chains is a determining factor in this characteristic. Strong polyelectrolytes become fully ionized when in solution and therefore maintain a strong surface charge over a wide range of pH. Weak polyelectrolytes are only partially ionized when in solution and therefore have a relatively weak surface charge. Furthermore, the concentration of ionized side-chains can vary depending on the pH, which affects the surface charge of such polyelectrolytes. Adjusting the pH and ionic strength of the solution allows for the manipulation of these films to swell, shrink, burst or release bound substances.[38]

Synthetic vs. Natural Polyelectrolytes

Polyelectrolytes can also be classified into synthetic and natural polyelectrolytes, which corresponds to how they are produced. When the LbL method was first established, researchers mainly used synthetic polyelectrolytes such as poly(allylamine hydrochloride), sodium polyacrylate, poly(diallyldimethylammonium chloride), and sodium poly(styrenesulfonate) for layer fabrication. Their physical and chemical properties are more reproducible than their natural counterparts and they have been widely studied since the early days of LbL synthesis.[33,39] Most of these polymers contain an aliphatic chain composed of carbon-carbon single bonds and as a result, they show a very low degradation rate once inside the body. However, this also means they are very robust, and they can withstand a wide range of pH, oxidant concentration and other factors. The most common side groups present on these polymers are carboxylates, sulfonates and amine groups[39] and this can be seen in the structures of common synthetic polyelectrolytes shown in Figure 2.5

Synthetic Polyelectrolytes

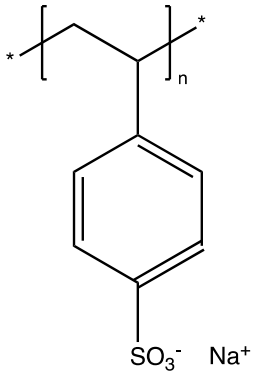

Sodium poly(styrenesulfonate)

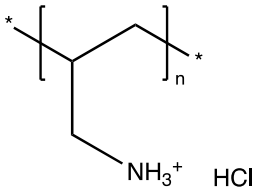

poly(allylamine hydrochloride)

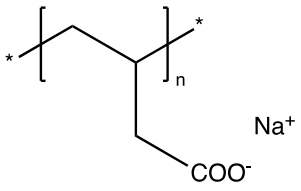

sodium polyacrylate

Natural Polyelectrolytes

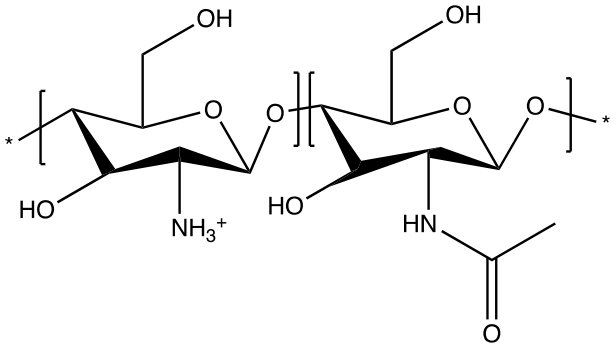

Chitosan

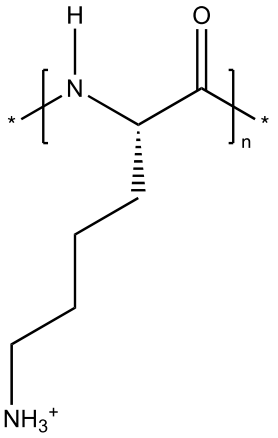

poly-L-lysine

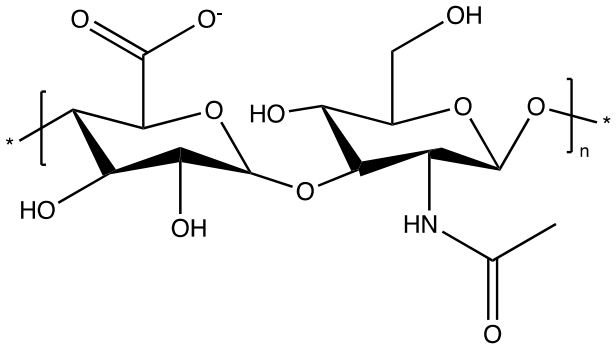

Hyaluronate

Figure 2.5: Chemical structures of common synthetic and natural polyelectrolytes

In recent years, the focus in biomaterial synthesis has shifted towards biocompatibility and biodegradability, and as a result, LbL fabrication has been adapted towards using natural polyelectrolytes. Natural polyelectrolytes are found in living organisms and can either be isolated and purified from their sources or synthetically produced in the lab. Examples of polyelectrolytes harnessed from natural sources include chitosan, alginate and hyaluronic acid whereas proteins and DNA can either be isolated from sources or synthesized from their monomers in a lab.[35,40] The process of extraction and purification of natural polymers can vary between different batches and suppliers and as a result, reproducibility can be an issue in studies. The chemical structures of common natural polyelectrolytes are outlined in Figure 2.5. Since natural and synthetic polyelectrolytes both have their advantages, their use in LbL coatings is contingent on the desired application.

2.4.2 Coating strategies

Layer deposition protocols can vary depending on the desired product, the nature of the substrate as well as the type of polyelectrolyte used. Several methods for layer deposition exist with the main ones including immersive, spin, spray, microfluidic and electromagnetic coating. This versatility allows for the application of the LbL technique in an array of fields. As discussed in previous sections, natural polyelectrolytes are more sensitive to their environment and prone to degradation unlike synthetic polyelectrolytes. Furthermore, the size, topography and nature of the substrate onto which the layer is deposited can influence the protocol used for coating. For instance, spin and spray coating procedures are used primarily on 2D substrates, whereas immersive, microfluidic and electromagnetic coating can be utilized for both 2D as well as 3D substrates.[4]

Immersive coating

Shortly after discovery, the methodology used for the synthesis of LbL constructs involved immersing planar substrates in the choice of polyelectrolyte and washing off any excess coating to repeat the process with the oppositely charged polyelectrolyte. This process is relatively fast and can be automated using robotics leading to efficient large-scale production. Time of incubation during coating is correlated with the adsorption kinetics of the polymer onto the substrate and it is expected to vary between different materials. It is also known that longer incubation period can produce thicker layers.[4] Although immersive coating was initially used only for planar substrates, it also allows for the coating of colloids and other 3D surfaces by incubating them in a solution containing the chosen polyelectrolyte. The excess polymer can subsequently be removed via centrifugation, filtration or other isolation methods. However, the additional steps required in isolating the coated substrate can reduce yield and also become laborious and time consuming for applications that require high number of bilayers.[41,42]

Spin-coating and spray-coating

Spinning and spraying techniques allows for quickest application of LbL coating compared the other methods. As a result, they can be repeated many times to synthesize finely organized macroscopic films with up to hundreds of bi-layers.[4] Spray coating involves using aerosolized polyelectrolytes, which are directly sprayed onto the substrate to create well-organized nanometric films that can be formed as fast as 6 seconds per layer. It surpasses all the other techniques in terms of being able to coat very large substrates that would otherwise be inefficient or impossible to coat via other methods, especially at an industrial scale. On the other hand, spin-coating requires an apparatus that affixes the substrate, which is spun continuously while a fine jet drips the

polyelectrolyte solution. As standard spin-coaters are available in many labs, this can be a facile and easily accessible technique in comparison to spray coating.[38] Asides from the differences in the coating apparatus, both spin-coating and spray-coating allow for thinner and more consistent coating in contrast to immersive protocols while using small amounts of liquid.[22] However, they also restrict the choice of surface to only planar, 2D surfaces and makes it difficult to coat complex, 3D surfaces.[20]

Electromagnetic coating

LbL coating using electromagnetic approaches can exploit either electric or magnetic fields. The former is based on the principles of electrodeposition, which is an established technique commonly used to create metal coatings on substrates. It involves the manipulation of ions (polyelectrolytes in this case) using an electric field towards a charged electrode, creating a fine coating. The latter approach uses magnetic substrates which can be manipulated through a solution of polyelectrolytes to coat them. Despite the requirements for complicated instrumentation, electrodeposition is a faster process than immersive technique and can coat a variety of shapes and surfaces including porous substrates.[43] On the other hand, magnetic approach is favoured in applications where the substrates are too small and difficult to isolate, such as quantum dots and other metallic nanoparticles whose diameter is 10 nm or under. Additionally, the process can be automated, which simplifies the process and reduces the hands-on-time.[4,20]

Microfluidic coating

Microfluidic devices have a wide-range of uses in biomedical engineering, including the synthesis of LbL coatings. The platforms allow for the use of laminar flow or capillary forces to

manipulate very small samples of polyelectrolyte.[35] Since these platforms allow for the manipulation of small quantities of fluids, they are extremely efficient in applications where the substrate or polyelectrolyte are very expensive or in limited quantity. Furthermore, these platforms can be used to cultivate and coat cells as well as other sensitive samples. Since the substrates can be trapped within the channels while the flow and incubation of polyelectrolyte solution creates the coating, it greatly reduces the chances of flocculation by avoiding harsher separation techniques such as centrifugation.[4,38] Additionally, the introduction of multiple channels allow for efficient scale-up of the process or high throughput screening of a large library of LbL constructs.[38] In summary, the variety of methods for layer deposition allows for tunability in forming these thin films on different geometries and surfaces This is further illustrated in Figure 2.6, which compares the different LbL coating techniques discussed above.

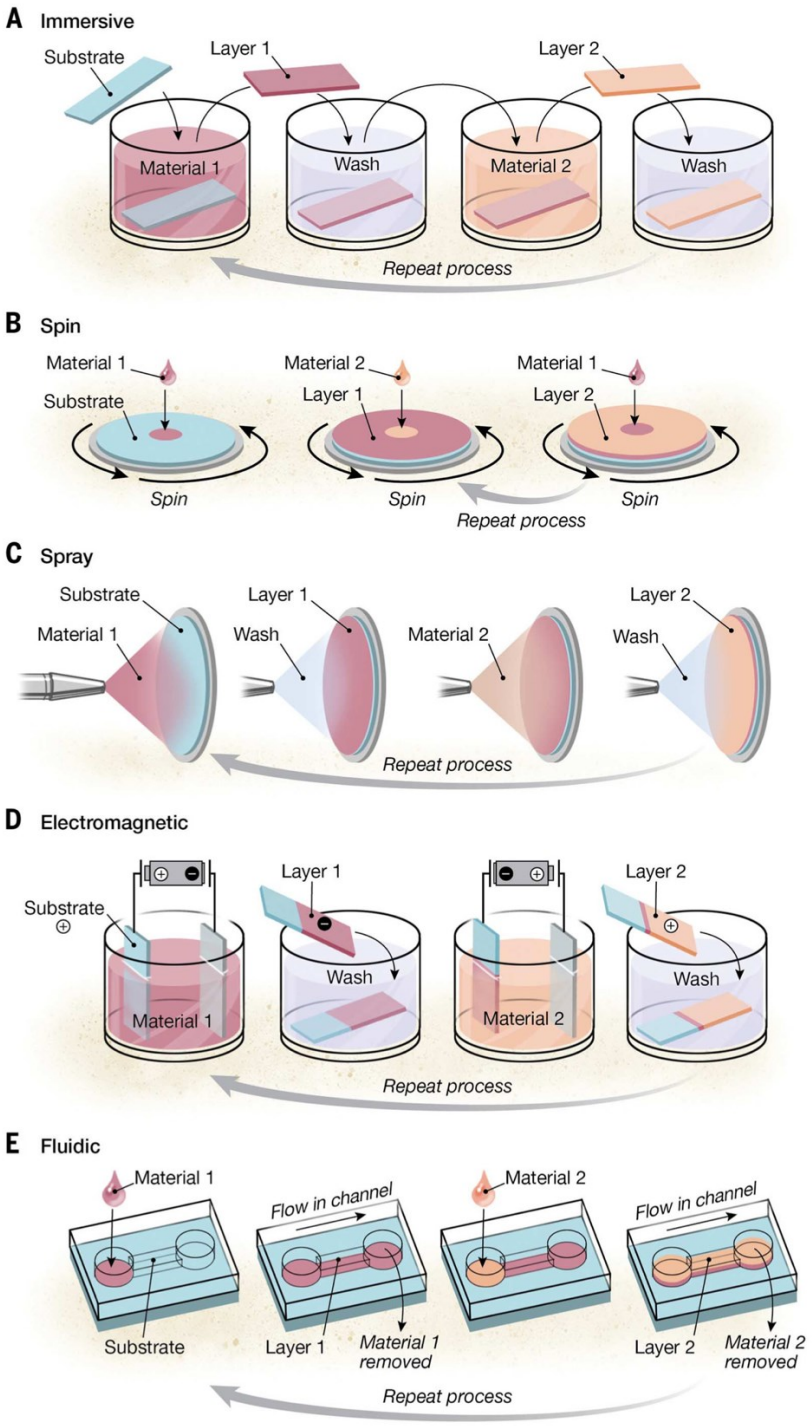

Figure 2.6: Schematic showing the different methodologies used to create multilayer assemblies via layer-by-layer self-assembly. Adapted from ref [4] with permission from AAAS [Illustration credit: Alison E. Burke and Cassio Lynm]

2.4.3 Characterization

There are several techniques available for film characterization and both qualitative as well as quantitative data about LbL films can be derived by using a combination of methods. Efficient and precise techniques to measure properties such as layer thickness, porosity, stiffness, surface roughness and stability are crucial in the characterization of LbL films. Furthermore, fast and versatile ways to monitor layer growth contribute to the simplicity of developing these films as well as their ability to incorporate a variety of 2D and 3D surfaces.[4,38] Outlined below are some commonly used instruments/methodologies for the characterization of LbL films.

Spectroscopy

Spectroscopy techniques allow to extract quantitative data about layer formation and chemical composition on 2D surfaces.[38] Examples include UV/Vis, X-ray photoelectron spectroscopy (XPS), and Fourier transform infrared spectroscopy (FTIR). As their names suggest, each method exploits electromagnetic waves at a specific wavelength: Ultraviolet/Visible, X-ray and infrared light. UV/Vis spectroscopy allows for the measurement of absorbed or reflected light in the ultraviolet/visible range assuming the adsorbed material is transparent and has specific absorption bands.[38,44] Absorbance is calculated using the Beer-Lambert law (Equation1) and changes in the absorbance signal is correlated with the composition of the adsorbed material and increase in absorbance can be expected with the increased deposition of layers.[45] On the other hand, XPS is able to provide data on the atomic composition of the polyelectrolytes,[44,46] while FTIR can be used to monitor film growth as well as the interactions taking place on the surface of the films by measuring vibrational energy of chemical bonds.[38,42,47]

$$A = log_{10} \frac{I_o}{I} \qquad \textbf{(1)}$$

Optical techniques

Surface plasmon resonance (SPR) and ellipsometry are commonly used optical techniques for characterization of film thickness, adsorption and other related properties onto 2D surfaces. SPR is a phenomenon describing the oscillation of electrons in the conductive band of metal surfaces, typically gold or silver. The deposition of materials on such metal surfaces directly affects the oscillation wave and binding events can be characterized with high sensitivity using this sensing platform. Binding kinetics and layer thickness can also be measured using SPR and the technique also allows for in-situ analysis of samples.[48,49] On the other hand, ellipsometry measures the change in polarization of transmitted/reflected light onto a thin surface. It can measure the thickness of LbL films and can be used to calculate the adsorbed mass of polymer using the refractive index along with thickness of material.[50] The technique requires that samples have to be dry, which is not favoured for samples that cannot/should not be dried as it can be detrimental to the material. Drying LbL films also reduces their thickness dramatically when compared with the hydrated film and therefore, it does not provide an accurate representation of the film thickness as well as its macrostructure.[22,38]

Quartz Crystal Microbalance with Dissipation (QCM-D)

Recently, QCM-D has become popular for precise characterization of LbL films on 2D surfaces as a diverse set of materials can be analyzed in solution/ native state. QCM measurements rely on a quartz crystal, usually coated with gold, that can be actuated using a power source to achieve the resonance frequency of the material. This resonance frequency can change based on the deposition or removal of mass from the sensor. As a result, the deposition of each layer can be measured using such device with nanogram sensitivity by converting this change of frequency to

mass using the Sauerbrey equation (Equation 2).[38,44] Furthermore, QCM-D apparatus measures the energy dissipation to determine the viscoelasticity of the sample, which allows for more sophisticated measurements of film physical properties.[22] Overall, it is a highly sensitive benchtop tool for in-situ measurement and tracking of layer growth as well as mechanical properties on any substrate.[4,44,46]

$$\Delta f = -\frac{2{f_o}^2}{A(\mu_q \rho_q)^{1/2}} \Delta m \qquad \textbf{(2)}$$

Zeta-potential

Zeta-potential measurements are used to determine the surface charge of a substrate, especially colloidal materials. The technique relies on the double-layer theory, which was initiated by Helmholtz in 1879 and modified by Stern in 1924 to model charge distribution around a particle in water with the presence of counter ions. The theory states that as the distance from the surface of the particle increases, the electric potential first shows a linear decrease up to a fixed distance known as the stern layer. The counter ions adsorbed to the surface of the particle within the stern layer are fixed. Outside of the stern layer lies the diffuse layer, where there is an exponential decrease in electric potential as distance from the surface increases. Furthermore, the counter ions present in this layer have more motion as the distance increases. Therefore, the distance at which counterions transition from immobile to mobile is described as the slipping plane (Figure 2.7) and zeta-potential is the electric potential of a surface at this distance. While measuring the electric potential directly at the surface could be more interesting, it is very difficult to obtain in experimental settings. As a result, zeta-potential measurements have been deemed as an excellent alternative strategy to quantify surface stability of colloids.[34]

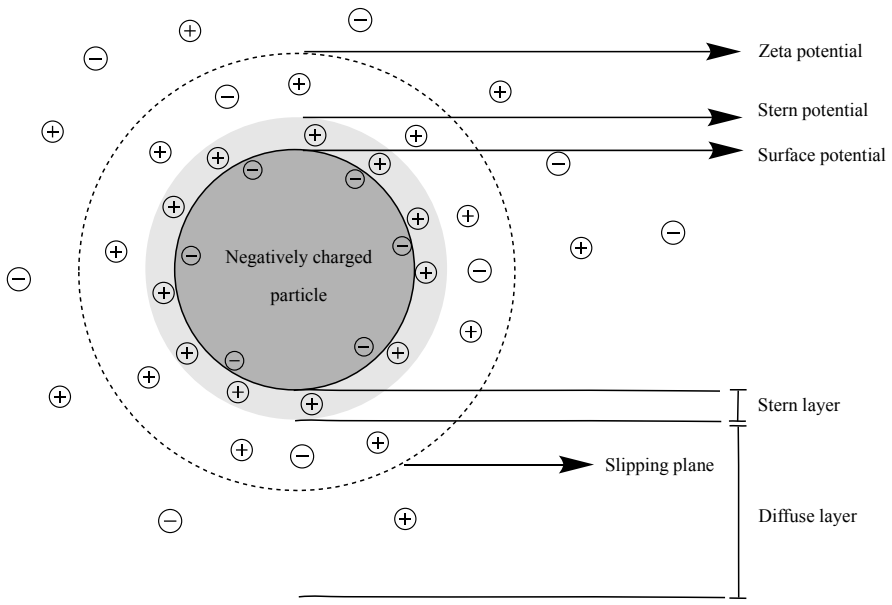

Figure 2.7: Illustration of the double layer theory for a negatively charged particle in aqueous solution.

Zeta-potential measurements can generally be obtained by using electrophoresis and measuring the migration of particles within the electric field using an optical detection system such as light scattering. The signal from the movement of particles causes a frequency shift, which is then expressed as electrophoretic mobility. The Henry Equation (Equation 3) is then used to calculate zeta-potential (ζ) from electrophoretic mobility (μ_E). Zeta potential values up to ±30 mV in magnitude describe neutral or weak-charged systems that are prone to flocculation, whereas zeta potential values greater than ±30 mV in magnitude have a strong surface charge and good stability in solution. Zeta potential analysis provides a quick way to track the surface charge reversal of a substrate, and therefore able to verify layer deposition, especially in 3D systems.[47,51]

$$\mu_E = \left(\frac{2\varepsilon\zeta}{3\eta}\right) f(\kappa r) \qquad \textbf{(3)}$$

High-resolution microscopy

High resolution microscopy is an excellent tool for characterization of layer morphology as well as size, porosity and permeability of both 2D and 3D substrates. Both transmission electron microscopy (TEM) and scanning electron microscopy (SEM) allow for high resolution measurements of layer thickness as well as porosity with nanometer resolution.[6,7,52] Atomic force microscopy (AFM) can also be used to evaluate layer morphology as well as viscoelastic properties of the polymer.[53] Confocal laser scanning microscopy (CLSM) can be used for 3D visualization of film construction as well as for studying the permeability of the LbL films by using fluorescent probes with various sizes and shapes (particles, long-chain polymers, hydrophilic vs. hydrophobic molecules).[54] Depending on the type of sample, one or more of these methods can be employed for physical and chemical characterization of the films.[22,38]

Mechanical properties

Assessment of the mechanical properties of LbL films such as stiffness and permeability as well as thermal properties can be achieved using a variety of techniques such as dynamic mechanical analysis (DMA) and differential scanning calorimetry (DSC) for 2D substrates, and AFM for both 2D and 3D substrates.[38,55] DSC can be used to measure differences between the melting point of polymer complexes and their individual constituents, which can be used to confirm complex formation. Changes in enthalpy and free energy of complex formation can also be derived from calorimetry measurements. DMA can be used to measure viscoelastic properties, glass transition temperatures and stiffness.[55,56] Both DSC and DMA require a substantial amount of the LbL construct for measurements, whereas AFM can be used to study mechanical properties such as Young's modulus and stiffness with very small quantity of sample.[38,42]

2.4.4 Applications of layer-by-layer self-assembly

As mentioned in previous sections, the application of layer-by-layer self-assembly started on planar macroscopic surfaces as it presented an opportunity to incorporate biocompatible coatings for biological applications. This can range from macroscopic implant surfaces like stents and bone substituents to cell culture plates and slides. The main purpose of this was to provide biocompatibility and decrease rate of attack by host immune system while increasing biointegation of the material. Furthermore, this can be extended to embedding drugs into the layers for slow release upon implantation.[57,58]

One good example of LbL coating on macroscopic samples is the work done by the Tabrizian group (Thierry *et al.* 2003) that investigated the use of chitosan/hyaluronan bilayers to coat and improve the bioactivity of NiTi stents.[58] This was done to combat in-stent restenosis, which occurs after a collapsed blood vessel is implanted with a stent and presents with excessive inflammation. NiTi alloy was pre-coated with polyethyleneimine and then up to four bilayers of chitosan/hyaluronan was deposited onto the metal substrate using the immersive coating technique mentioned earlier. This treatment resulted in a pronounced decrease of contact angle, which increases surface wettability and biocompatibility. Furthermore, platelet adhesion assay showed increased thromboresistance as a result of decreased platelet adhesion on the treated surface when compared with untreated metal. The polymer bilayers were also tested as a drug delivery system for encapsulating sodium nitroprusside, which is often used to combat in-stent restenosis. The incorporation of the drug within the stent surface not only provides targeted delivery to its active side but also showed increased thromboresistance in the assays previously discussed when compared with both bare metal as well as metal with non-drug loaded coating.

Another benefit of this technique is its ability to incorporate a wide variety of biocompatible polymers for coating. This includes polysaccharides such as chitosan and alginate, proteins, DNA and such. The use of biocompatible polymers allows for the technique to be utilized in developing coatings onto micro and nano-scale substrates in medical applications. A good example of this is displayed by the work done in Hammond's group (MacDonald *et al*. 2011) towards developing an LbL film for controlled BMP release in-vivo.[59] BMP-2 is a growth factor often used as a therapeutics towards bone regeneration and its controlled release is significant owing to the fact that bone regeneration is a slow process. The film included a multilayer system composed of BMP-2, a cationic poly-beta-aminoester and chondroitin sulfate. Their results showed a slower release of BMP-2 with the LbL construct compared to commercial collagen matrices and improved differentiation of progenitor cells for bone regeneration in *in-vivo* models.

The Tabrizian group (Mansouri *et al.* 2011) also investigated LbL coating for cell encapsulation, specifically the encapsulation of red blood cells to provide immunocamouflaging effect in the synthesis of artificial universal blood.[6] Bilayers of alginate/chitosan-graft-phosphorylcholine were surrounded by bilayers of alginate/poly-l-lysine-graft-polyethylene glycol and the encapsulated cells were tested to ensure that they function normally. Oxygen uptake and cell viability of the encapsulated cells were found to be similar to non-coated control cells. Furthermore, agglutination studies that expose the cells to antibodies that recognize blood surface-antigens show that the coated cells remain without aggregation. This serves as proof that the encapsulation provides a good resistance against recognition by these antibodies and therefore showing great promise to be used as a universal blood substitute with little to no immune reaction. A graphical representation of all the applications discussed here is illustrated in Figure 2.8.

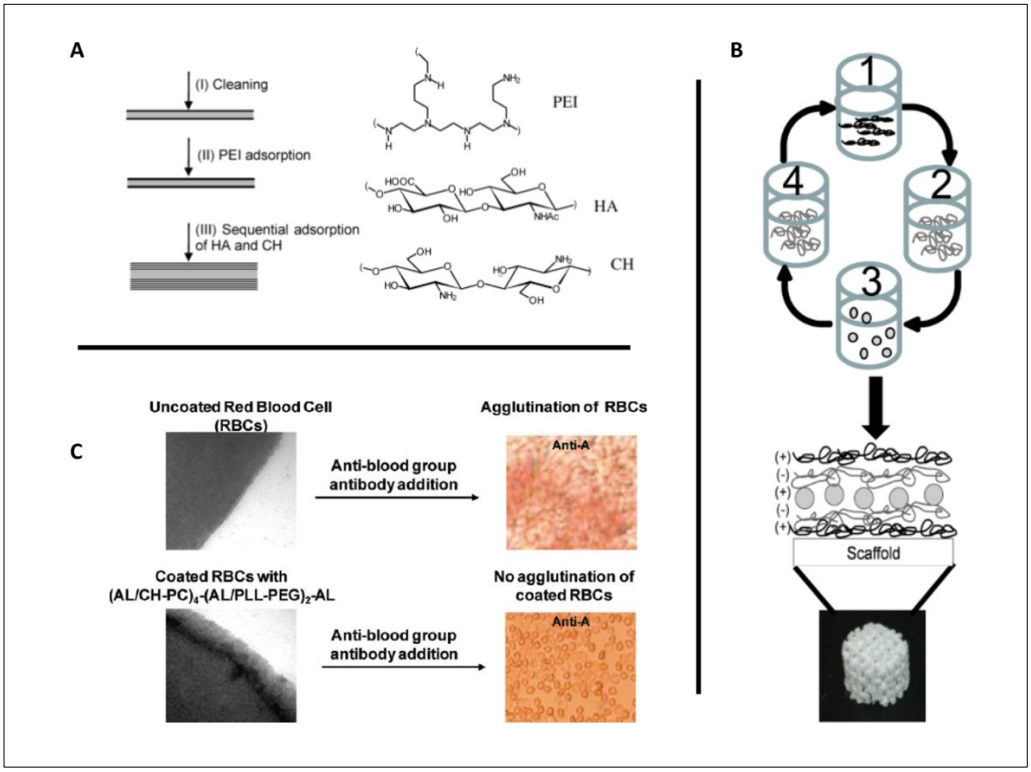

Figure 2.8: Illustrations describing LbL applications found in the literature from the works of Thierry *et al.* 2003 (A) [Image reproduced with permission from ref [47], Copyright 2003 American Chemical Society]; MacDonald *et al.* 2011 (B) [Image reproduced from ref [48], Copyright 2011 with permission from Elsevier] and Mansouri *et al.* 2011 (C) [Image reproduced with permission from ref [6], Copyright 2011 American Chemical Society]

These examples show the wide variety of applications LbL coatings can have, from implant surface treatment to drug release and cell encapsulation. Research in the field is still growing and the use of LbL towards new approaches in drug delivery and regenerative medicine are prevalent.[35] As the versatility of the method is clearly demonstrated by the examples provided in this section, the proposed thesis project aims to explore an unprecedented application of LbL in fabricating hollow capsules using live cell templates and natural polyelectrolytes, which is discussed hereafter.

2.5 Live cells as template for preparation of hollow capsules

The use of cells as template for the preparation of hollow capsules can widen the possibility of incorporating various morphologies, sizes and shapes. It could also incorporate materials already encapsulated within the cell as cargo. Some examples in the literature include the use of red blood cells and bacteria cells as a template due to the relative simplicity of such cell types. The ability to pre-load these cells with the cargo that can later remain encapsulated within the hollow microspheres represents a similar ideology as using oil droplets as templates but with the added benefit to include both hydrophilic as well as hydrophobic entities.[1,60–62] In the proposed study, *E. coli* will be used as the sacrificial template as these cells are well-studied and characterized in the literature. Furthermore, they are easy to culture, manipulate and maintain.

2.6 Materials used in proposed study

2.6.1 *E. coli*

Escherichia coli DH5alpha (abbreviated as *E. coli* DH5α) is chosen as the model substrate for this study. *E. coli* is a gram-negative bacteria, owing to the fact that it possesses very little peptidoglycan cell wall in its membrane compared to its gram positive counterparts.[63] It's a rod-shaped bacteria often found in the intestine of animals as well as within the environment. DH5α is a specific non-infectious clone of *E. coli* that is not present in nature and only used in laboratory research. It contains genetic mutations that encode for blue-white screening in plasmid recombination and lower endonuclease degradation to promote plasmid transfer. Overall, it is a reasonably safe strain of bacteria that allows for easy maintenance and manipulation and as a result makes experiments straight forward and trouble-free.[64]

The cell contains an outer wall composed of a lipopolysaccharide, followed by a periplasmic space with peptidoglycan and an inner cytoplasmic membrane as shown in Figure 2.9. Aside from this, the inside of the cell only contains a cluster of genomic material and ribosomes. This lack of organelles or other cell structures translates to a relative simplicity in comparison to eukaryotic cells that have many types of organelles, cytoskeleton and other intracellular structures. The relative simplicity of this cell makes it ideal for a sacrificial template. The cell membrane can be disrupted by dissolution of the membrane lipids using mild detergent based lysis buffers, which should be not harmful towards the polymer encapsulation.[37,63,65,66]

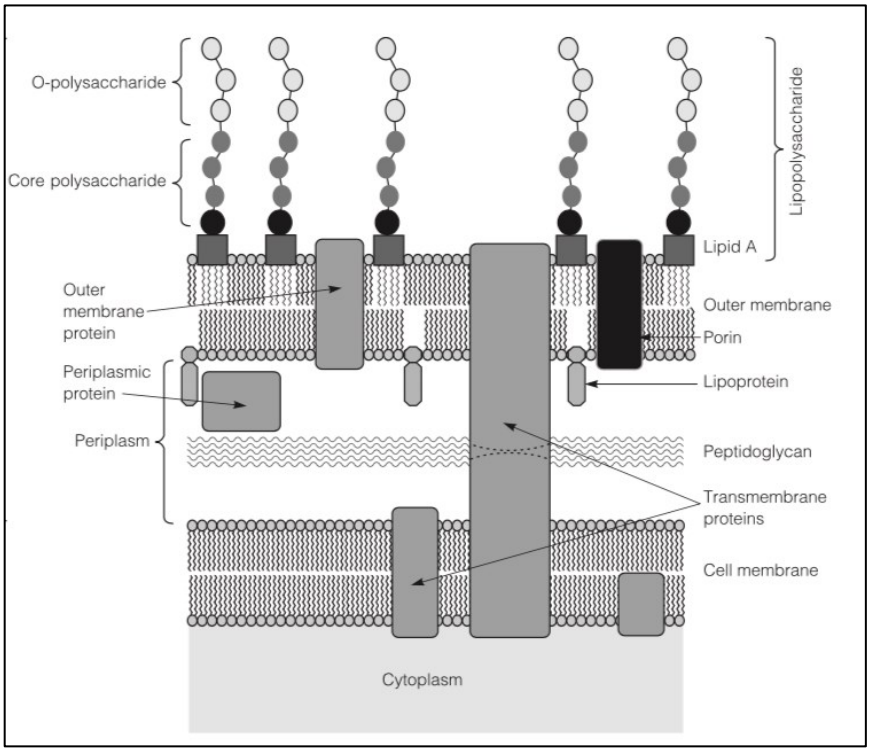

Figure 2.9 : Structure and organization of *E. coli* cell membrane. Image adapted from ref [52] Copyright (2011). Reproduced by permission of Taylor and Francis, a division of Informa pl

The breakdown and dissolution of cell material will be investigated as cell debris will need to be washed away to create free standing membranes or hollow capsules.[4] This will require

exposing the coated cell to a solution that does not damage the film but will lyse the cell. Researchers have used sodium hypochlorite and other lytic reagents to achieve this.[1] However, the use of biocompatible polymers will require mild conditions for cell lysis. The ability to control swelling and porosity of these membrane allows for the dissolved substance to wash out from the core creating a free-standing capsule.[4]

Protocols for the lysis of *E. coli* cells are well-established in microbiology and molecular biology as *E. coli* is a powerful tool for the study of recombinant proteins, genes, etc. Most of these protocols look to destroy most of the cell component with the exception of their target molecule (protein, DNA or membrane lipids).[63,67] This is achieved by disrupting the hydrophobic interaction in the outer membrane using detergents or alcohols and digesting the peptidoglycan layer using lysozyme.[68,69] DNase or other enzymes and enzyme inhibitors can be added to degrade unwanted components or protect the target molecule from self-degradation via the released enzymes from the bacteria itself. Furthermore, some studies incorporate glycerol and other substances as stabilizers for protein extraction. While this describes the general idea behind cell lysis, specific protocols operate in different mechanisms and identifying the right lysis protocol that is suitable for the application is imperative. For example, some detergent-based protocols use SDS, which is an ionic detergent and can intercalate with other charged molecules. This can disrupt the proposed layer-by-layer assembly and therefore must be substituted by a non-ionic detergent such as Triton-X or Tween. Furthermore, the use of heat or high concentration of divalent salts such as $MgCl_2$ and $CaCl_2$ are also common techniques in cell lysis for protein extraction and the preparation of competent cells but they can be detrimental to the proposed multilayer coating.[66,70,71] Overall the aim of this project with respect to cell lysis is to protect the layer-by-layer construct and all other cell macromolecules like DNA, protein can be degraded or washed away.

2.6.2 Natural polyelectrolytes

Biocompatibility has been a big focus in the field with the switch towards using natural polyelectrolytes such as chitosan, hyaluronic acid and such for LbL encapsulation.[72] As a result, these materials are an important focus to the proposed study. Chitosan and alginate are used to form the capsules, both being from natural sources, biodegradable and contain a polysaccharide backbone. Polysaccharides are correlated with intrinsically high chain stiffness[54] which should make them more stable than linear aliphatic chains. Furthermore, the isoelectric points of their side chains allow us to manipulate their properties within the physiological range. The stability and thickness of the films formed with such systems can be adjusted by manipulating pH, temperature and ion concentration as discussed earlier.

Chitosan is a linear polysaccharide obtained from chitin, an abundant component of shell fish exoskeleton. The linear structure is composed of a mixture of β(1-4)-linked N-acetyl-D-glucosamine and D-glucosamine groups. Chitosan is produced via deacetylation reactions on chitin in basic conditions, which removes the acetyl groups from N-acetyl-D-glucosamine on the polymer to leave an exposed amine group (Figure 2.10). The yield of this reaction is represented as degree of deacetylation and can be easily verified by NMR and commercially obtained chitosan often has this information stated in the product sheet. Higher degree of deacetylation (>90%) is usually favoured as that corresponds with a high concentration of free amine group, which provide a strong positive charge on the polymer once they are protonated. The pKa of this free amine group is 6.5 and as a result, chitosan has to be dissolved in acidic solutions. However, once dissolved, it can be titrated up to its pKa and still stay in solution. Its most common use in the medical field is

as a hemostatic agent, component for hydrogels and other biomaterials, and also relevant in LbL applications.[73,74]

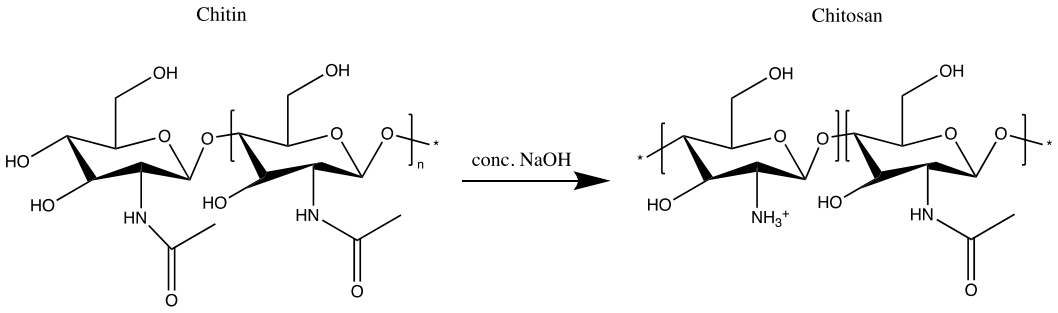

Figure 2.10: Reaction scheme for the deacetylation of chitin in basic conditions to produce chitosan.

Alginic acid, commonly referred to as alginate, is extracted from cell walls of brown algae and often present as salts of sodium or calcium after processing. It is a linear polysaccharide just like chitosan, but it is composed of (1-4)-linked-β-D-mannuronate and α-L-guluronate (Figure 2.11). The two monomers are considered epimers, therefore sharing the same chemical identity and structure with a difference in configuration at only one stereocenter. The polymer is widely used in food and pharmaceutical owing to its excellent property in absorbing water.[75] Alginate has a negative charge in neutral pH with a pKa of 3.5. Therefore, it maintains its surface charge around physiological pH.[76] Both polymers are biocompatible, widely studied and relatively inexpensive, which make them excellent candidates for capsule material in this study.

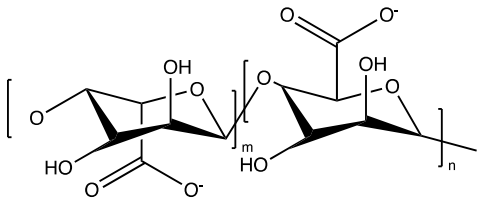

Alginate (m - gluronate, n - maluronate)

Figure 2.11: Chemical structure of alginate monomers.

2.6.3 Buffer system

A buffer solution consists of a weak acid and its conjugate base or a weak base and its conjugate acid, which is then able to sequester any added acids or bases in order to maintain the pH of the solution at a fixed value. The Henderson-Hasselbalch equation (Equation 4) describes the correlation between the concentration of acid and base components of the buffer and its pKa in determining the pH of a buffer.[37] Choice for buffer system is important for two major reasons: cell survival and maintaining the integrity of the capsule. As the surface charge on the polymers depends on the pH in which they are subjected to, it is important to pick a buffer that can match the pH which will result in the optimal surface charge for the polymer. Furthermore, this also has to be suitable to the physiology of the bacteria to avoid any shock response or sudden death of cells during the coating protocol. There are a few good options for buffers in physiological range such as phosphate buffered saline (PBS), tris(hydroxymethyl)aminomethane (TRIS), acetate, and citrate.[66] However, the buffering capacity of these buffers are different for a given pH due to their different pKa and their ionic strengths are also different. For example, PBS has a multivalent anion with a charge of -3 and therefore has a higher ionic strength for the same concentration in comparison with acetate, which has a monovalent anion with a charge of -1. As a result, a suitable buffer will be determined experimentally by assessing the stability of the multilayer construct in different buffer conditions.

$$pH = pK_a + log_{10}\frac{[A^-]}{[HA]} \quad \textbf{(4)}$$

2.6.4 Quantum dots

Quantum dots are used as a proof-of-concept cargo, since it is easy to embed them within the microcapsules and track them during synthesis and characterization by various techniques. They are highly fluorescent, semiconducting nanocrystals with various composition that show high stability in comparison with traditional fluorophore molecules. Their fluorescence properties are size-dependent and they have a narrow emission spectra, which makes them favourable amongst biologists in multiplexed immunofluorescence studies.[71] Their uptake in eukaryotic cells is mediated by endocytosis mechanism, which is widely established in the literature. On the other hand, the uptake of QDs in prokaryotic cells such as *E. coli* is achieved via induced cell competence, which is often applied for the uptake of small plasmids into *E. coli*. Due to the presence of an outer membrane, peptidoglycan layer and cytoplasmic membrane on the surface of *E. coli*, cell competence by using $CaCl_2$ achieves physicochemical disruption of the cell membrane structures and allows for internalization of substances into the *E. coli*.[71,77,78]

3. MATERIALS AND METHODS

3.1 Materials

Chitosan (MW=100,000-300,000 Da, ~90% deacetylation) was obtained from MP Biomedicals. Sodium Alginate (MW=150,000 Da) and Quantum Dots (CdSeS/ZnS, λ_{em}=630 nm, 6 nm diameter, 1mg/mL in toluene) were obtained from Sigma-Aldrich. Phosphate buffered saline (PBS) tablets (1X), Luria-Bertani (LB) broth powder, Luria-Bertani (LB) agar powder, sodium chloride and methanol were all obtained from Bioshop. Polystyrene microspheres (3μm and 5μm in residual SDS) were obtained from Phosphorex. Glycerol, acetic acid, potassium monohydrogen phosphate, potassium dihydrogen phosphate, hydrochloric acid and fluorescein isothiocyanate (FITC) were all obtained from Sigma-Aldrich. Sodium hydroxide, sodium acetate, and ethanol were obtained from Fisher Scientific. Polystyrene cuvettes (4X optically transparent) were purchased from Malvern. Triton-X and glutaraldehyde were obtained from Fluka Analytical. Aqua-Mount® was obtained from Lerner Laboratories. Sodium cacodylate buffer, osmium tetroxide, acetone, Epon ® and uranyl acetate were all obtained from various venders and used without further purification. LIVE/DEAD® BacLight™ Bacteria Viability Kit was purchased from Molecular Probes. Ultra-pure water (MilliQ) from a Barnstead filtration system (resistivity above 18.2 MΩ-cm) was used for all experiments.

3.2 Bacteria cell culture protocol

Media preparation

Liquid growth media was prepared by dissolving LB-broth powder (10g tryptone, 10g NaCl and 5g yeast extract for 1L of media) into mQ water and autoclaving immediately at 121℃ to sterilize. Once sterile, liquid media was kept at room temperature and periodically tested to ensure sterility by incubating an aliquot of the media into the incubator overnight and checking for any growth of bacteria. Agar plate media was prepared in a similar fashion by dissolving LB agar powder into mQ water and autoclaving immediately at 121℃. After the media has cooled back down to ~50℃, it was poured into 15 mm petri dishes and stored in the fridge until use. Control plates/broth media were used at all times during cell culture to ensure no contamination has occurred to the broth media as well as the agar plates.

Cell culture protocol

Stock *E. coli* DH5α cells, which were stored in glycerol at -80°C, were streaked on 4% agar plate and grown in a shaking incubator overnight at 37°C. A single colony was scraped and used to inoculate 3 mL of sterile LB broth in 15 mL round-bottom Falcon tube to be used as a starter culture. This culture was grown overnight in a shaking incubator at 37°C until stationary phase (OD_{600nm} ~1.5). 1 mL was taken from this culture to inoculate a 50 mL sterile LB broth in a 125mL Erlenmeyer flask and the cells were grown in a shaking incubator at 37°C until OD_{600} of 1.0 was reached and these cells were used for subsequent experiments. Cell density was determined using plate reader and measuring the absorbance of the sample at OD_{600}.

3.3 Preparation of polyelectrolyte solution

Chitosan solution was prepared by dispersing chitosan powder into water using a round-bottomed flask and a magnetic stirrer. 10% acetic acid was added while the sample is stirring at high speed until the solution had a final concentration of 1% acetic acid and 10 mg/mL chitosan solution. The dispersion in water was done first to prevent the clumping of chitosan, which occurs when large amounts of chitosan powder comes into contact with acetic acid. The solution was stirred overnight and subsequently pH balanced with 1M NaOH and dilute to 1mg/mL or 3 mg/mL depending on the experiment. The solution was then filtered using 0.2 μm PES syringe filters before storage.

Alginate was dissolved either in water or the corresponding buffer used for the reaction at 10mg/ml under high stirring in a round bottom flask. Its pH was balanced using 1% acetic acid. The solution was then diluted to 1 mg/mL or 3 mg/mL depending on the experiment and filtered using 0.2 μm PES syringe filters prior to use. Both polyelectrolytes formed clear solutions and were kept at room temperature in polypropylene falcon tubes wrapped with aluminum foil to avoid UV degradation.

3.4 Preparation of buffers

Each buffer system (PBS, Tris, Acetate) was prepared at room temperature using deionized water. The Henderson-Hasselbalch equation was used to calculate how much of the individual acid/base component is needed to make the specific buffer at a given pH and these components were then mixed with the water. The pH of the buffer is measured and titrated accordingly using either 1M HCl or 1M NaOH until the desired pH is obtained. All buffers formed clear solutions and were filtered using 0.2 μm PES filters and kept in polypropylene tubes at room temperature.

3.5 Synthesis of FITC-labeled chitosan

FITC-labeled chitosan was prepared as described by Ma *et al.*[79] and shown by the reaction scheme in Figure 3.1. Briefly, 200 mg of chitosan was dissolved in 10 mL of 1% AcOH and an equal volume of methanol was added into the solution for a final concentration of 10 mg/mL. FITC (2 mg/mL) was then added at ratio of 1:15 (w/w) (FITC:Chitosan) and the reaction ran for 18 hours in the dark under N_2. Once the reaction was complete, the chitosan was precipitated by adding 1M NaOH and vacuum filtered until the supernatant was clear and pH neutral. Fluorescent intensity was also measured to ensure negligible amount of unreacted FITC was present in the wash supernatant. The fluorescently labeled chitosan was freeze-dried and stored at room temperature in the dark until further use. For LbL coating, FITC-chitosan was dissolved at 3 mg/mL, pH balanced and filtered using 0.2 μm PES syringe filters as per the protocol mentioned earlier for the preparation of chitosan solution.

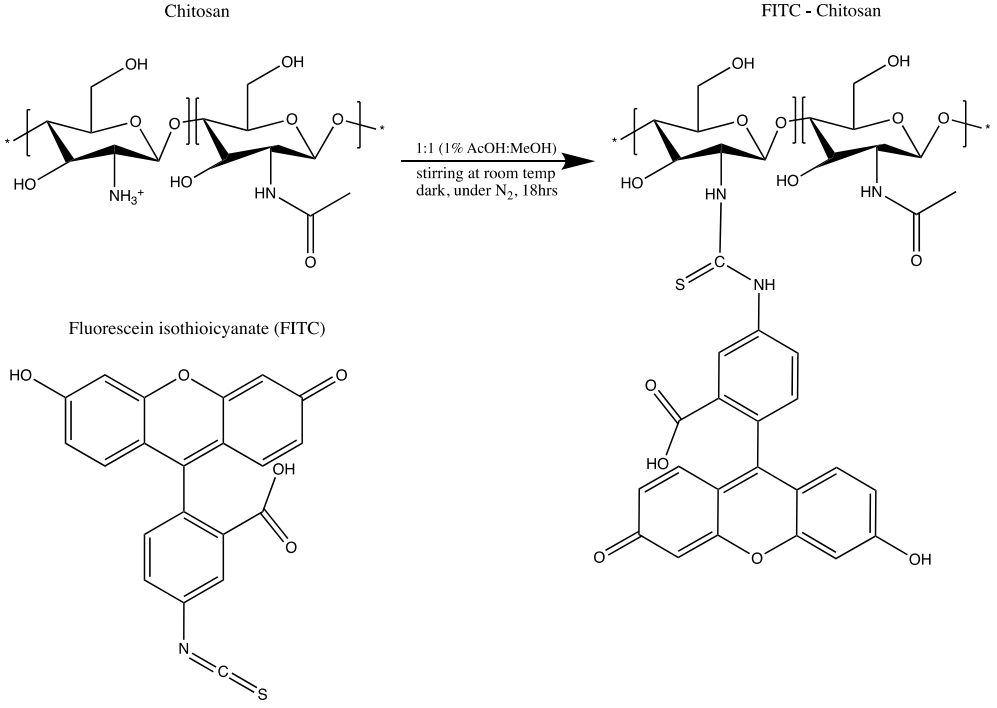

Figure 3.1: Reaction scheme for the coupling of fluorescein isothiocyanate (FITC) onto chitosan.

3.6 Synthesis of LbL-coated materials

Synthesis of multilayer coated polystyrene microspheres

Polystyrene microspheres particles (5 μm) were washed to remove excess surfactant by centrifuging at 4000 rpm for 5 mins. The particles were dispersed in deionized water to a total concentration of 1 mg in 2 mL by vortexing for 5 sec intervals and zeta potential measurements were taken before coating with polyelectrolytes. 200 μL of 1 mg/mL chitosan was added into the solution and the particles were vortexed for 5 sec to mix and gently agitated for 20 mins on a shaker. Afterwards, they were centrifuged at 4000 rpm for 5 mins and supernatant was replaced with deionized water. Zeta potential measurements were obtained, and the particles were subsequently coated with 600 μL of 1 mg/mL alginate in the same fashion. The coating steps were repeated until six to eight layers were achieved.

Synthesis of multilayer coated fixed *E. coli* cells

Once the *E. coli* cells reached the desired concentration in their growth phase (OD_{600} ~ 1.0 or $1x10^9$ cells/mL), they were harvested by centrifugation at 4000 rpm for 15 mins. The cells were washed 3x in phosphate buffer (10 mM, pH 5.8 with 0.1M NaCl) and spun at 4000 rpm for 10 mins. They were fixed using 2.5% glutaraldehyde in PBS (pH 5.8) at an OD_{600} of 0.35 (~$2.8x10^8$ cells/mL) by incubating for 2 hours in the fridge. Once the fixation was done, the cells were washed 3x in water to remove the glutaraldehyde and used for coating procedure. The cells were dispersed into a 50 mL polypropylene tube at ~$3x10^8$ cells/mL and a total volume of 9.5 mL. For LbL coating, 500 μL of 3 mg/mL chitosan solution was added into the cell suspension for a total volume of 10 mL and the mixture was vortexed for 5 secs and incubated for 20 mins. The cells were then centrifuged at 3000 rpm for 5 mins and the supernatant was replaced with fresh buffer. 150 μL of

3 mg/mL alginate was then pipetted into the cells to form the subsequent layer and the procedure was repeated until the desired number of layers was obtained.

Synthesis of multilayer coated live *E. coli* cells

Once the *E. coli* cells reached the desired concentration in their growth phase (OD_{600} ~ 1.0 or $1x10^9$ cells/mL), they were harvested by centrifuging at 2300g for 10 mins. The cells were washed 3x in acetate buffer (10 mM, pH 5) and spun at 2300g for 6 mins before being re-suspended in acetate buffer to an OD_{600} of 0.35 (~$2.8*10^8$ cells/mL) in a 50 mL polypropylene tube. 500 μL of 3 mg/mL chitosan solution was added into 9.5 mL of cell suspension and vortexed for 5 secs. The mixture was agitated for 20 mins on a shaker at room temperature and excess polyelectrolyte was removed by centrifuging at 1600g for 5 mins and resuspending the pellet in 7.85 mL of acetate buffer. 150 μL of 3 mg/mL alginate was then added to deposit the next layer in the same fashion as chitosan. The process was alternated until the desired number of bilayers were achieved with the outermost layer being alginate. A general outline of the LbL procedure used in this study is outlined below in Figure 3.2.

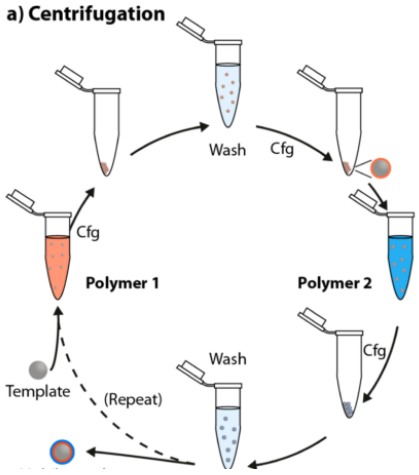

Figure 3.2: Schematics of LbL coating onto particles/cells using the immersive method used in this study. Image reproduced with permission from ref [36]. Copyright 2013 American Chemical Society.

3.7 Cell lysis protocol

Once the LbL coating procedure was completed, the samples were immediately incubated with the lysis buffer of choice at the same total volume used to perform the coating. This was done to maintain the cell concentration and avoid any aggregation as a result of concentrating the cells prior to the lysis procedure. The cells were incubated either in 1% Triton-X buffer with 2 mM EDTA or 50% isopropanol solution for 12 hours. After the incubation period, the samples were washed 4x with acetate buffer to remove the detergent and subsequently prepared for TEM or confocal microscopy imaging using protocols mentioned below.

3.8 Quantum dot encapsulation

Quantum dots (1 mg/mL) were diluted to 0.2 mg/mL in Triton-X (2% in 10 mM acetate buffer, pH 5) as a working concentration right before encapsulation. *E. coli* cells were grown until they reached near stationary phase (OD_{600} ~ 1.0 or $1x10^9$ cells/mL) and harvested by centrifuging at 2300g for 10 mins. The cells were washed 3x in acetate buffer (10 mM, pH 5) and spun at 2300g for 6 mins before being re-suspended in acetate buffer to an OD_{600} of 1.0 in a 50 mL polypropylene tube. Quantum dots added into the cell suspension to a final concentration of 20 μg/mL and mixed by pipetting up and down several times before they were allowed to incubate for one hour under shaking at room temperature. Afterwards, the cells were washed 3x by centrifuging at 2300g for 6 mins to remove any quantum dots left within the suspension. The cells were then used immediately for coating experiments or other characterization procedures. LbL assembly onto QD-labeled cells was carried out per the procedures outlined above.

3.9 Confocal microscopy

Samples were labeled using FITC-chitosan and alginate for confocal microscopy to indicate the deposition of the polymer onto the cells. Nuclear staining (Hoechst 33323) was also used to co-localize nuclear material and characterize cell lysis as the two dyes (FITC and Hoechst 33323) have discrete emission spectra and can be superimposed. After LbL coating, the sample was incubated with Hoechst 33323 at a final dye concentration of 10 μg/mL for 30 mins and washed 3x using acetate buffer. 20 μL of the sample was then mounted onto a glass slide using Aqua-Mount® and a coverslip before imaging. Confocal images were obtained using a Zeiss LSM-710 microscope. Image analysis was done on Zeiss image processing software provided with the microscope as well as on Image-J software.

3.10 Zeta-potential analysis

Samples were diluted 1/3 for zeta-potential by adding 500 μL of sample into 1mL of buffer or water to keep the electrolyte concentrations consistent. Sample was prepared in transparent polystyrene cuvettes (10x10x45 mm) and measurements were taken using Brookhaven Zeta PALS DLS. The PALS (phase analysis light scattering) function allows for using lower electric fields to obtain measurements, which can reduce Joule heating in samples with physiological salt concentrations. The software was set to have 5 sweeps/run and 10 runs per sample to ensure consistent values are being obtained as per suggestion from the equipment manual. The zeta potential of the substrate's surface is calculated by measuring the electrophoretic mobility of the sample as described in the introduction (section 2.4.3) and the Zeta PALS software computes the values of zeta potential based on that equation. Statistical analyses of the results were performed on Microsoft Excel® and represented as graphs in the result section.

3.11 Transmission electron microscopy

Once cells were coated with the desired number of layers, the acetate buffer is removed via centrifugation (3000 rpm for 5 mins) and replaced with 2% glutaraldehyde solution. The cells are fixed for two hours and the solution is replaced with fresh buffer and kept overnight. The next day, the cells are washed 3x with cacodylate buffer for 5 mins with centrifuge at 5000 rpm to ensure pellet doesn't resuspend for subsequent steps. After the wash, samples are stained with osmium ferricyanide and left in the fridge to incubate for 2 hours. This is followed by washing with water 3x before the sample is dehydrated using a series of washes using acetone to water solutions (30%, 50%, 70%, 80%, 90% and 3x100%). The pellets are then incubated with a solution of Epon ® : Acetone (1:1, 2:1, 3:1 and 100%) over a 3-day period at room temperature. The sample is then dried under vacuum for 2 hours and polymerized at 60°C in an oven for 48 hours. Afterwards, the samples are cut under a microtome, embedded into carbon coated grids and stained using 2% uranyl acetate. TEM images were obtained using a Tecnai 12 BioTwin 120kV microscope.

3.12 Cell viability assay protocol

Cell viability assays were conducted using a LIVE/DEAD® BacLight™ Bacteria Viability Kit from Molecular Probes and the protocol provided from the supplier. Cells were diluted to a concentration of $2x10^8$ cells/mL and live cell samples were incubated in buffer while dead cell samples were incubated in 70% IPA for one hour, mixing every 15 minutes. Afterwards, five sets of 2 mL samples were prepared in glass vials with various ratios of live:dead cells (0, 10, 50, 90 and 100% live cells) by mixing the appropriate amount of live and dead cells. 6 μL of each stain (12 μL total) were added into 2 mL of mQ water in a glass vial to create a working solution of the stains. 100 μL of the cell samples were pipetted into a 96-well plate in triplicate along with 100

μL of the working solution. The samples with the pre-determined ratio of live cells were used to make a standard curve by plotting the ratio of fluorescence intensity of the live-cell stain (SYTO® 9, λ_{em}=530 nm) over the fluorescence intensity of the dead-cell stain (propidium iodide, λ_{em}=630 nm) against the percentage of viable cells in the sample. This plot was used to determine the viability of experimental samples by obtaining live/dead ratio values and using them to calculate cell viability.

4. RESULTS

4.1 LbL assembly on polystyrene microparticles

Layer-by-layer assembly was first attempted on polystyrene microparticles to optimize the protocol for concentration, coating conditions and other factors. The polystyrene particles were 3-5 μm in diameter and chosen because they were in a similar size range as the *E. coli* cells used in this study (~2μm). The concentration of particles optimal for LbL assembly was determined based on values adapted from the literature[6] and adjusting the number of particles proportionally to maintain the total surface area of the particles/ml the same as the literature values. This step was crucial in order to minimize aggregation and maximize stability of the layers. The stock particles (2.5% w/v) were purchased with a concentration of $5x10^8$ particles/mL and were used at a concentration of 1 mg/3mL ($6.7x10^6$ particles/mL)

Since the particles has a weak surface charge, they were coated in pure milliQ water with no salts to reduce any charge shielding that could occur with the presence of salts. Due to the presence of stabilizing surfactants present in the stock microsphere solution, the particles had to be washed to reduce aggregation between excess surfactant and polyelectrolyte before LbL coating. The non-coated particles (layer 0) had a stable negative charge (-39.5±1.6 mV) after wash and dispersion in mQ water as shown in Figure 4.1. The deposition of chitosan (layer 1) caused the reversal of the surface charge to positive and this alternation of surface charge continues with subsequent steps, indicating the successful deposition of each layer.

Layer	Zeta-potential (mV)
PS (0)	-39.5±1.6
CHI (L1)	53.3±4.8
AL (L2)	-58.3±1.5
CHI (L3)	58.9±1.6
AL (L4)	-32.6±1.1
CHI (L5)	44.5±1.6
AL (L6)	-21.4±1.1

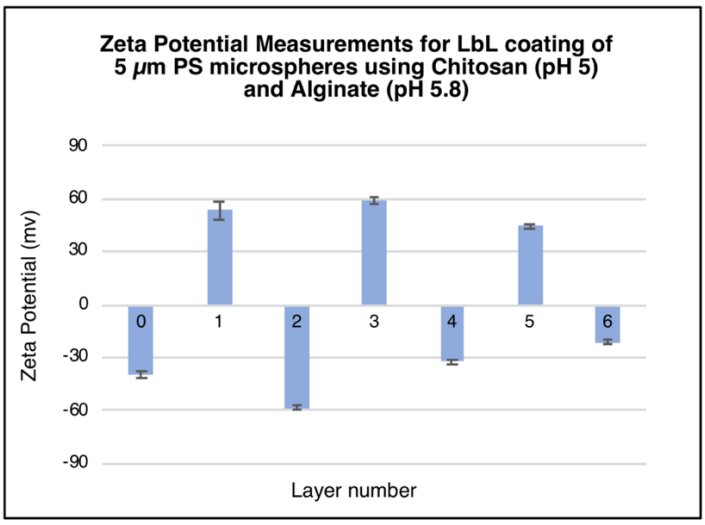

Figure 4.6: Zeta potential measurements tracking the layer deposition of chitosan and alginate onto 5 μm PS microspheres in mQ water. The scale on the graph highlights the threshold for stability of the system (±30 mV)

As the assembly reaches higher number of layers, a dramatic loss of mass occurred together with a significant decrease of pellet size, which was observed during centrifugation. This was expected as the repeated number of washes are known to reduce the yield of this assembly method with colloidal particles. This effect will likely become more pronounced as the number of layers increases, which is correlated with an increased number of washes and pipetting steps. As a result, the initial amount of substrate must be chosen accordingly in order to obtain enough yield of the final product for subsequent analysis such as staining protocols for microscopy.

4.2 LbL assembly on fixed *E. coli* DH5α cells

Once the coating protocol was established using polystyrene microspheres, fixed *E. coli* cells were used to further optimize the conditions. Fixing the cells with glutaraldehyde prior to coating allows for the manipulation of the cells for long duration without causing damage to the cells before the coating procedure is finished. It was found that unlike the polystyrene

microspheres, fixed bacteria suspended in milliQ water had a higher surface charge (-39.5±1.6 mV vs. -53.1±1.1 mV) as shown in Figure 4.2. This can be correlated with the abundance of surface proteins present on the bacterial cell wall, which would have a negative surface charge as most amino acid residues are negatively charged in neutral pH.[37] Furthermore, stable LbL films were created on fixed *E. coli* cells in water at pH 5.8 to ensure the pH stayed below the pKa of chitosan (pKa =6.5) and to maintain the polymer's positive charge.

Layer	Zeta-potential (mV)
Cells (0)	-53.1±1.1
CHI (L1)	36.6±1.0
AL (L2)	-44.6±1.2
CHI (L3)	28.5±0.9
AL (L4)	-45.6±1.8
CHI (L5)	26.5±1.0
AL (L6)	-61.6±1.8
CHI (L7)	32.2±1.0
AL (L8)	-48.9±1.2

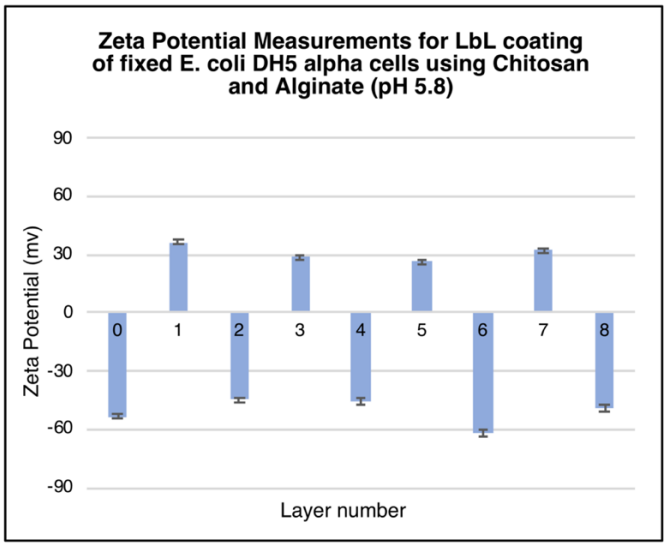

Figure 4.2: Zeta potential measurements tracking the layer deposition of chitosan and alginate onto *E. coli* cells fixed with glutaraldehyde (2%) in mQ water. The graph scale highlights the threshold for stability (±30 mV)

Concentration of cells is important factor to consider and this was determined by the same method as the calculations done earlier for polystyrene microspheres. A similar study done by Mansouri et. al determined that $1x10^7$ red blood cells/mL seem to give the least amount of aggregation in an LbL experiment with cells[6]. The total surface area of these cells was calculated and a similar total surface area on *E. coli* cells represents ~$3x10^8$ cells/mL. While this calculation is an approximation, it proved to be relatively accurate as shown in microscopy and zeta-potential

results. It was seen during experiments that higher cell concentrations did cause problems with aggregation.

Despite the reasonable stability of this system in water, it was important to be able to do this coating in a buffer system, as control over pH is important to maintain a stable physiological environment for the subsequent live cell experiments. A buffer system was used with a pH close to physiological pH while also acidic enough to retain chitosan in its dissolve state with sufficient surface charge to form a stable coating. Hence the samples represented in Figure 4.2 were coated at pH 5.8, which is as acidic as PBS can get while retaining its buffering capacity. Most buffers have to be used in a pH range of ±1 to maintain good buffering capacity, which occurs when both the acid and conjugate base are present in adequate quantity. This pH range establishes that at least 10% of either the acid or conjugate base in the buffer is present within the buffer as determined by using the Henderson-Hasselbalch equation. Anything outside of this range would not make a good buffer and since PBS has a pKa of 6.8, it can be effectively used as a buffer up to a pH of 5.8. These conditions were expected to cause major aggregation as a result of the reduced concentration of protonated amines on the surface of chitosan as pH gets closer to the pKa of its amine group. Despite this reduction in the surface charge of chitosan, the zeta potential analysis illustrated that the samples were rather stable.

The formation of aggregates was prominent when these cells were coated in buffers containing salts, which was a factor that required further optimization. NaCl as well as KCl are both common components in most physiological buffers to maintain osmotic pressure in cells as well as participate in the cell metabolic functions. However, it was found that the presence of these salts often leads to aggregation and as a result, the best buffer system was chosen as the one with

no added NaCl or KCl. The ionic strength of the buffer was significantly lower and therefore, much less charge shielding was observed with no added NaCl/KCl. This can be verified by the increase in zeta potential of the sample when measured in low salt buffers (Figure 4.3). It demonstrates that the absence of NaCl (0 mM) yields the highest surface charge and stability for non-coated cells as well as chitosan coating onto the cells. Additionally, it is observed during preparation of these samples that the cells coated with chitosan in buffer without NaCl form a well-dispersed cloudy solution after preparation, whereas the sample containing 100 mM of NaCl forms macroscopically visible aggregates that become difficult to re-disperse. This observation, complementary to the zeta potential measurements, indicate that the use of buffer without NaCl provides the best environment to create a well-dispersed and stable coated construct.

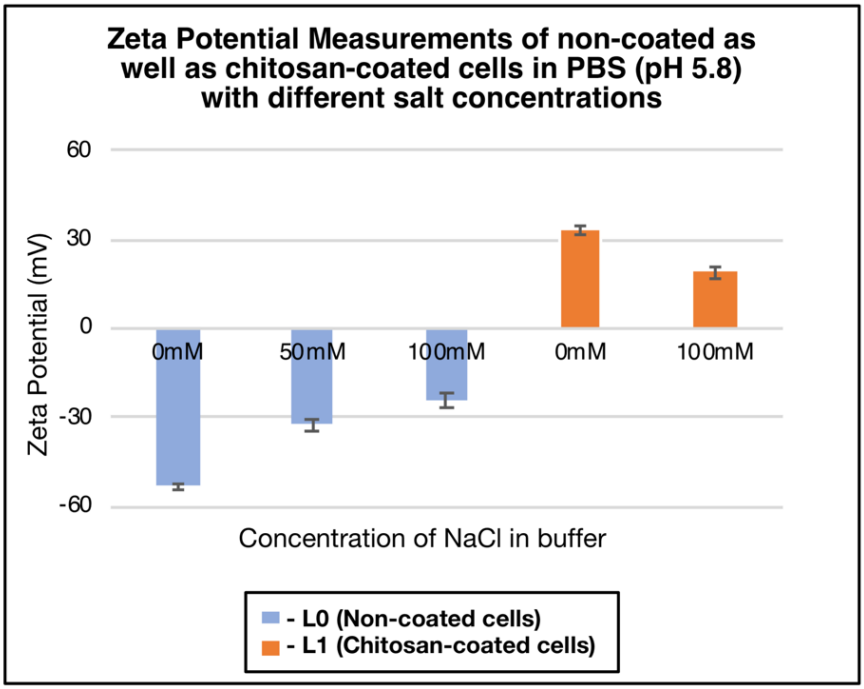

Figure 4.3: Zeta potential measurements of non-coated cells and chitosan-coated cells to measure surface charge in buffer with different concentrations of NaCl.

Fluorescence microscopy was used to show layer deposition onto the fixed cells by using chitosan conjugated with fluorescein isothiocyanate (Figure 4.4). This ensured that the chitosan is forming distinct polymer nanofilms on top of the cells and not present in bulk within the solution. It also allows for controlling aggregation and overall serves as a complementary characterization tool along with zeta potential to monitor layer deposition and stability. Zeta potential results of the coating with fluorescent chitosan showed a lower magnitude reading when compared with its non-fluorescent counterpart (data not shown). This was expected as the attachment of fluorescein molecules onto the chitosan backbone happens at the free amine groups that give chitosan its positive surface charge when protonated. Therefore, the presence of these fluorescent groups reduces the number of free amine groups on the polymer, which in turn reduces the surface charge.

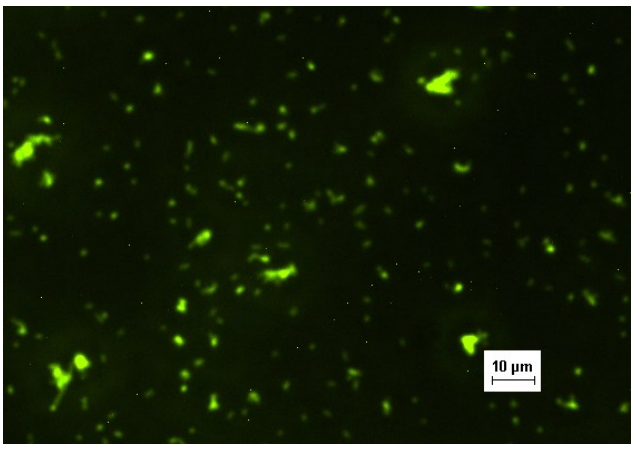

Figure 4.4: Fluorescence microscopy image of *E. coli* cells coated with fluorescein-conjugated chitosan

Several different buffers were tested for coating, and more stable microcapsules were obtained at pH 5 in comparison with pH 6 (by 10%). Also, the coating was most stable when no additional salts (NaCl, KCl) were present in the buffer. Following these results, acetate buffer was chosen as the ideal buffer since it provided the best buffering capacity at pH 5 based on its pKa in comparison to PBS and other commonly used buffers. While the addition of saline is important to

maintain osmotic pressure in the cells, the buffer with no salts seems to provide the most stable layer construct.

4.3 LbL assembly on live *E. coli* DH5α cells

Once all the factors were optimized, the coating was performed on live *E. coli* cells which were harvested around OD_{600} 0.8-1.0 near the end of exponential phase. These cells remain viable in acetate buffer (10 mM, pH 5) with no added salt and up to four bi-layers have been constructed using these cells. The zeta potential data shown in Figure 4.5 demonstrates good stability with each layer as well as the charge reversal that occurs as the cell is coated with a polycation followed by a polyanion. A decrease in pellet size was also observed in these experiments similarly to the experiments with PS microspheres. While higher number of layers can be fabricated by continuing this protocol, it was decided for this study that 4 bilayers were enough to formulate a stable capsule.

Layer	Zeta Potential (mV)
Cells (0)	-54.67±1.1
CHI (1)	30.28±1.29
AL (2)	-37.95±1.51
CHI (3)	40.05±0.93
AL (4)	-37.82±2.05
CHI (5)	36.95±1.93
AL (6)	-41.64±1.02
CHI (7)	43.58±1.16
AL (8)	-39.33±1.22

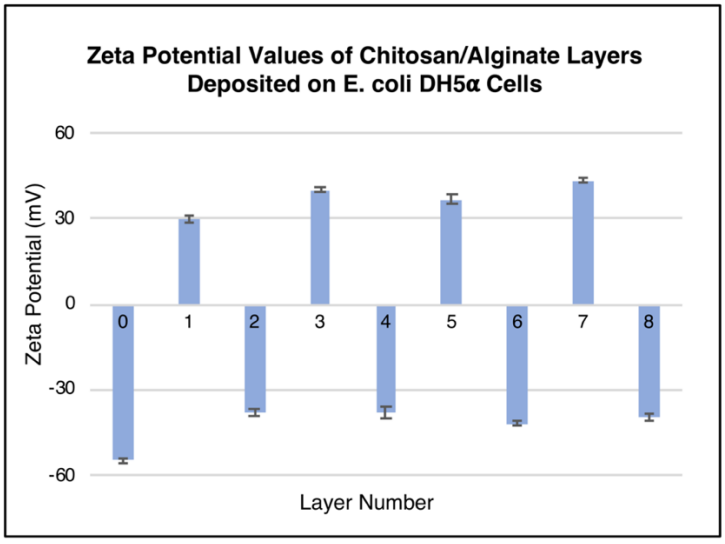

Figure 4.5: Zeta potential measurements tracking the layer deposition of chitosan and alginate onto live *E. coli* cells in acetate buffer (10 mM, pH 5). The scale on the graph highlights the threshold for stability (±30 mV)

Confocal microscopy images confirmed the layer deposition on live cells with minimized aggregation (Figure 4.6). Hoechst 33342 staining was used to localize DNA material and indicate that the cells are intact. Fluorescein-labeled chitosan allowed for the visualization of the layer deposited onto the cells. Furthermore, there was little to no aggregations of cells, which is favourable for the aim of this project. Subsequent lysis steps rely on the permeability of lysis agent within these samples as well as the flow of cellular debris out of the sample. As a result, severe aggregation would hinder this process.

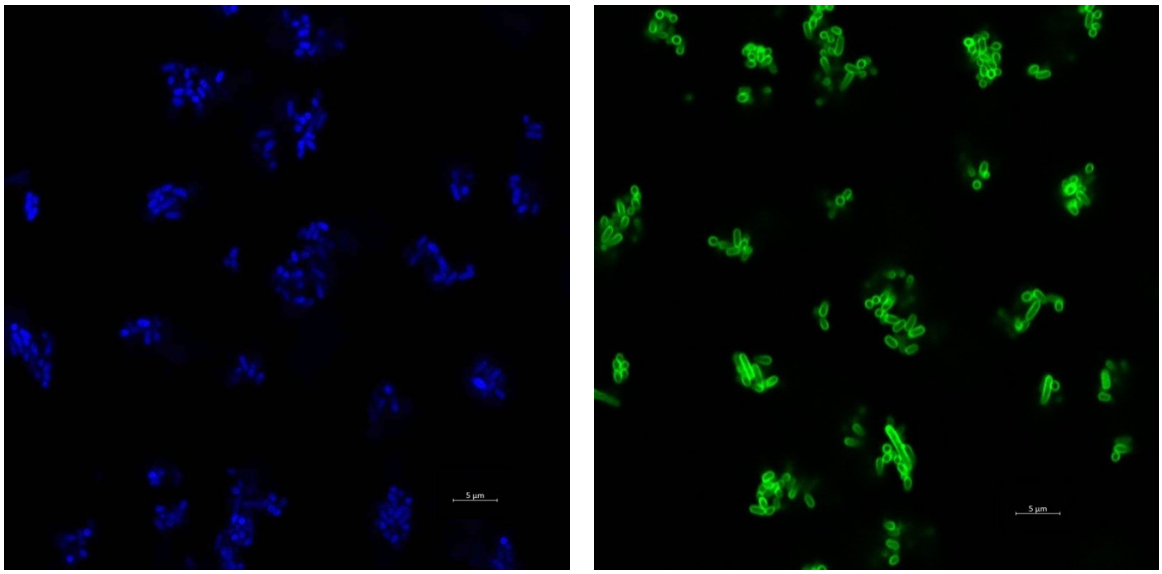

Figure 4.6: Confocal microscopy images of *E. coli* cells coated with FITC-labeled Chitosan (right) and control cells stained with Hoechst 33342 (left) (63x mag).

TEM images were used to characterize layer thickness and morphology with high resolution. The results are shown in Figure 4.7 where the chitosan/alginate membrane as well as the components of the bacteria cell membrane can be clearly outlined with nanometer precision. The thickness of the membrane formed with 4-bilayers of chitosan/alginate was found to be ~20 nm with the thickness of the bacteria membrane also ranging between 10-20 nm. This is consistent

for *E. coli* based on literature values.[80] The LbL membrane also shows to be tightly packed as it would be expected due to the lack of salt in the buffer. This lack of charge shielding causes the polyelectrolytes to have strong intrachain and interchain repulsion, resulting in a linear confirmation of the polymer chains.[47]

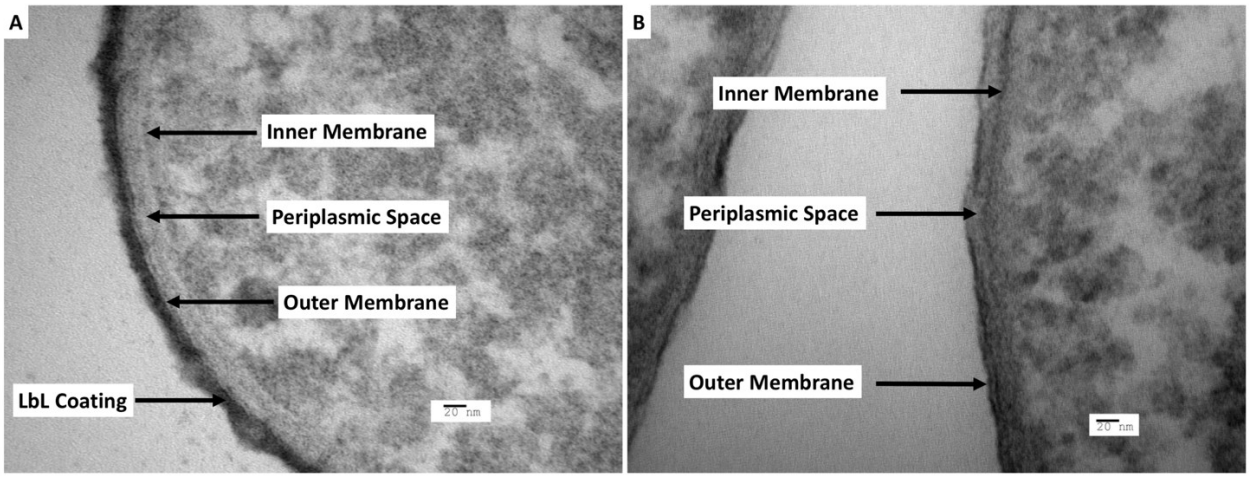

Figure 4.7: High magnification (98000x) TEM image of LbL coated *E. coli* with 4 bilayers of chitosan/alginate (A) and non-coated control cell (B). The image outlines the membrane components as well as the coating.

The differences between different number of layers was also investigated using TEM as shown in Figure 4.8. The higher number of layers resulted in a more organized and tightly packed membrane in comparison to coating with less layers (L4 vs. L8). The stability of the layers is expected to improve with increasing number of layers even though this is not evident in the zeta-potential data for live cell coating. According to literature, this is a result of increasing consistency in charge distribution on the previous layer and as the polyelectrolytes assemble on each other, they create an evenly charged surface and tightly bound layers.

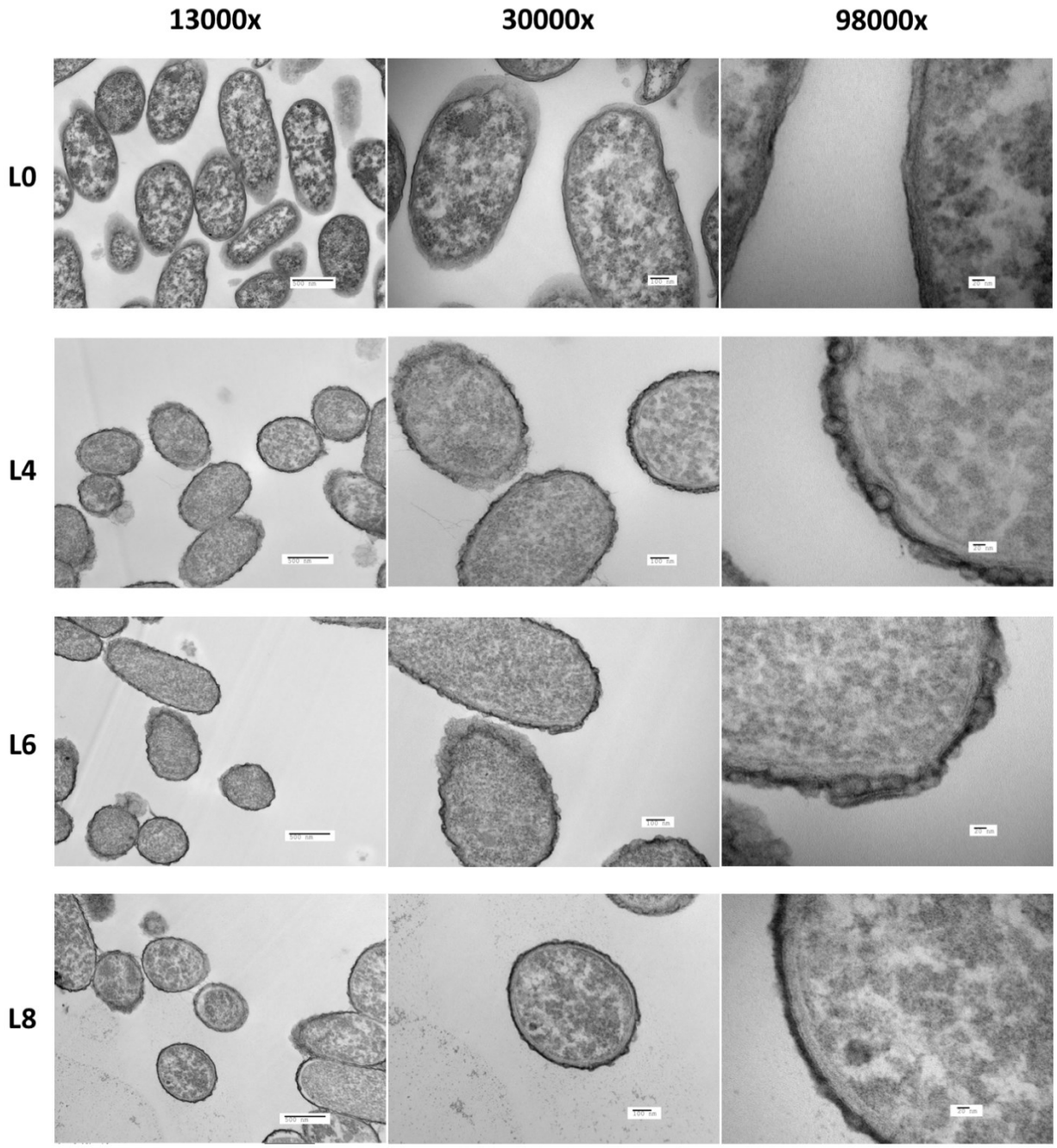

Figure 4.8: TEM images of non-coated *E. coli* cells (L0) and chitosan/alginate coated *E. coli* cells with four layers (L4), six layers (L6), eight layers (L8). Image magnifications are the same for each column and indicated at the top of each column.

4.4 Hollow microcapsules from LbL assembly on live *E. coli* DH5α cells

In order to generate hollow microcapsules from multilayer-coated cells, several conditions were tested for cell lysis including isopropanol, ethanol and detergent based (Triton-X) buffers. In each case, some cell destruction was witnessed but the focus was on determining which method results in the highest yield of hollow microshells devoid of any cellular components. When choosing cell lysis condition, it was important that the condition is harsh enough to kill the cells but mild enough to keep the capsule intact. Figure 4.9 shows hollow capsules, which are indicated by arrows, obtained from coated cells treated with either isopropanol (C) or lysis buffer (D).

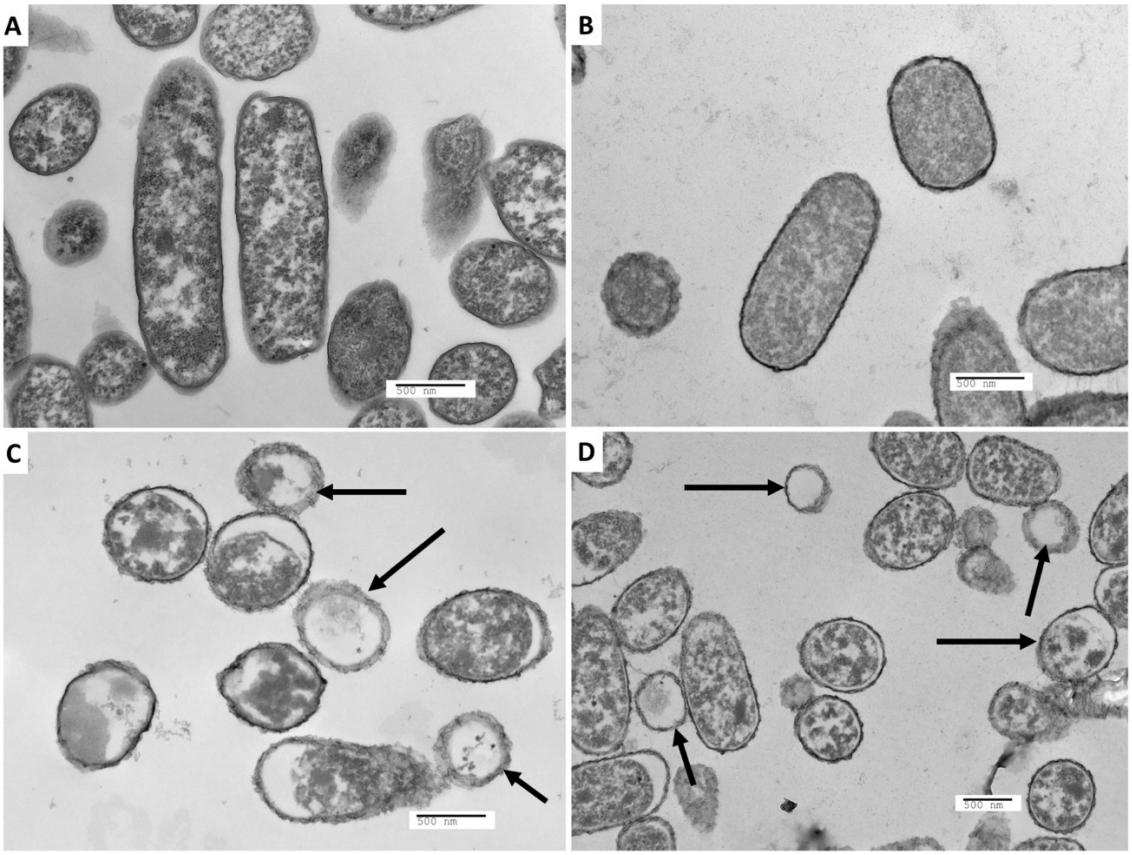

Figure 4.9: TEM images of non-coated control cells (A), coated cells with 4 bilayers of chitosan/alginate (B), hollow capsules prepared via exposure to isopropanol (C) and hollow capsules prepared via exposure to Triton-X based detergent solution.

Both lysis agents seemed to show similar yields in terms of cellular destruction to produce hollow microcapsules despite their different mode of action. The isopropanol works by rapidly dehydrating the cell, which causes the cell to burst by osmotic shock. Meanwhile, the detergent-based lysis buffer contains Triton-X, which is a non-ionic detergent that can solubilize lipids and other membrane components of the cell. EDTA is added into the buffer to chelate Mg^{2+} ions, which stabilize the membrane and therefore, their removal causes the membrane to break down. This is an established method in cell biology for protein and DNA extraction from bacteria and known to produce high yields for cell lysis.

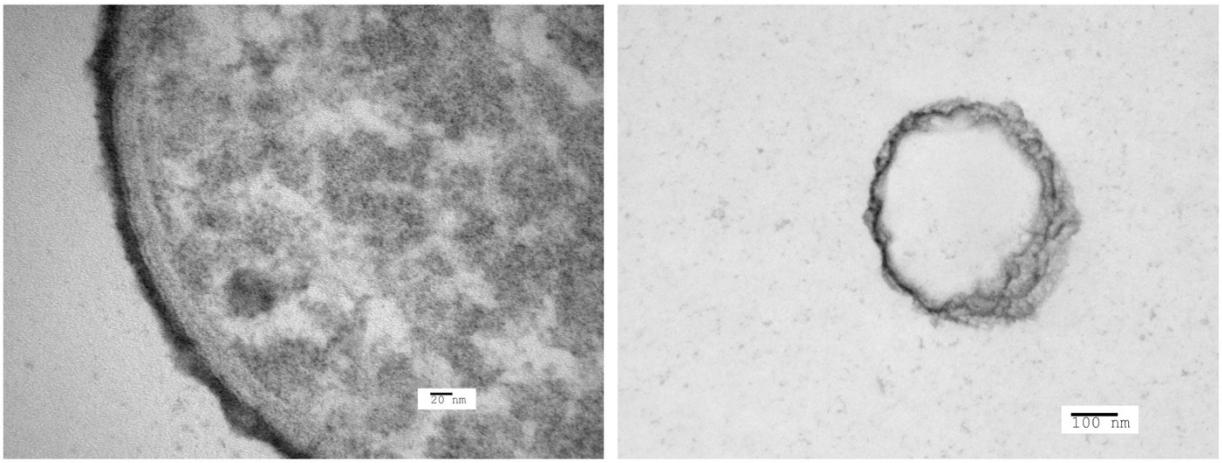

Figure 4.10: TEM images showing morphology and thickness of intact multilayer-coated *E. coli* (left) vs hollow multilayer microcapsules (right).

Using TEM also allows for the morphological characterization of hollow capsules, which are otherwise hard to differentiate in light microscopy due to limits in resolution. Figure 4.10 demonstrates that the microcapsules with complete removal of cell components show an increase in membrane thickness in comparison with intact constructs. This can be attributed to the relaxation of ionic bonds between the polymer due to the lack of mechanical support from the core.

It has been reported in the literature that hollow microcapsules can often deform and in some cases collapse once their core template is removed.[61]

4.5 Live/Dead Assay

Live-dead assay was also conducted to test the viability of the cells after harvesting as well as after coating. The premise of the live-dead assay is to quantify the cell integrity, which the assay accomplishes by measuring the degree to which the cell membrane is compromised. The two dyes used in the assay differentiate between live/dead cells as they have different affinities for internalization. Propidium iodide is only permeable in cells whose membranes are compromised, whereas SYTO 9 ® can penetrate both live and dead cells. The fluorescence of each dye can be measured using a plate reader and based on a standard curve, the viability of the cells can be calculated as a percentage as shown in Figure 4.11.

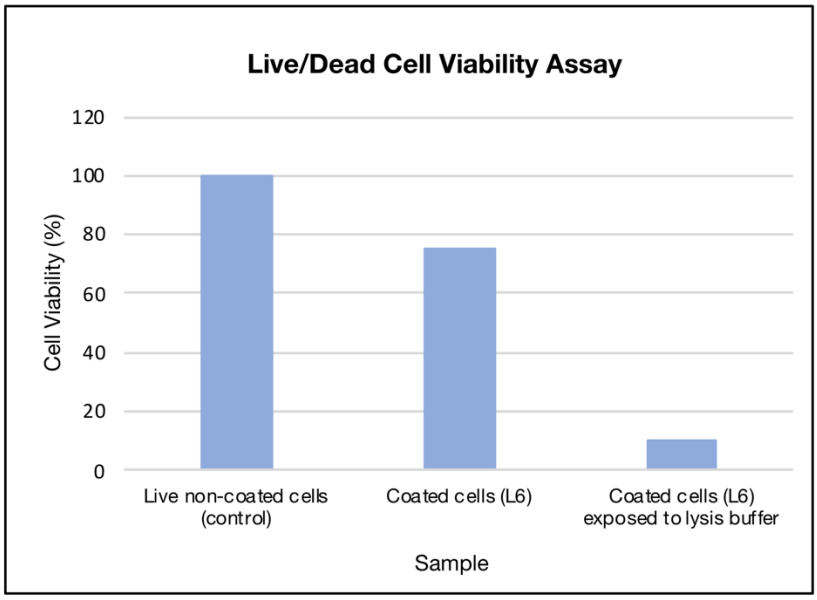

Figure 4.11: Cell viability measurements for live non-coated *E. coli* cells, cells coated with 3 bilayers of chitosan/alginate (L6) in acetate buffer (10mM, pH5) as well as cells exposed to Triton-X based lysis buffer.

As demonstrated in Figure 4.11, cell viability decreased to 75% for coated cells. This reduction in cell viability can be attributed to the rigorous steps that are involved in layer formation such as repeated pipetting, vortexing as well as centrifugation and to the coating itself. These steps can compromise the membrane integrity of the cells and this, in turn, will result in reduced cell viability based on this assay. Furthermore, the polymer coating on the cells can also be a contributing factor. Chitosan is widely reported to be an anti-microbial and disrupts the cell membranes of bacteria.[81] Despite this property of chitosan, only 25% of the cells had a compromised membrane and the cells generally show good viability.

While this measurement provides quantitative data on the viability of the cells as well as the coated constructs, it does not indicate whether or the cell components are broken down or have been cleared out of the polymer capsule. Since the goal of this study is to achieve this clearance, only TEM was used as a high-resolution characterization method, as mentioned in earlier sections, for the formation of these hollow microspheres.

4.6 LbL assembly on live *E. coli* DH5α cells labeled with Quantum Dots

Quantum dots (CdSeS/ZnS alloyed) were first incubated with *E. coli* cells before LbL assembly was undertaken. The uptake of QDs into the cells was confirmed by confocal microscopy (Figure 4.12) as the cells show strong fluorescence emission at 630 nm after successful encapsulation. The cells were also stained with Hoechst 33342 to co-localize the quantum dots with intracellular DNA. Furthermore, cells were coated with fluorescein-labeled chitosan to confirm LbL assembly onto the QD-coated cells.

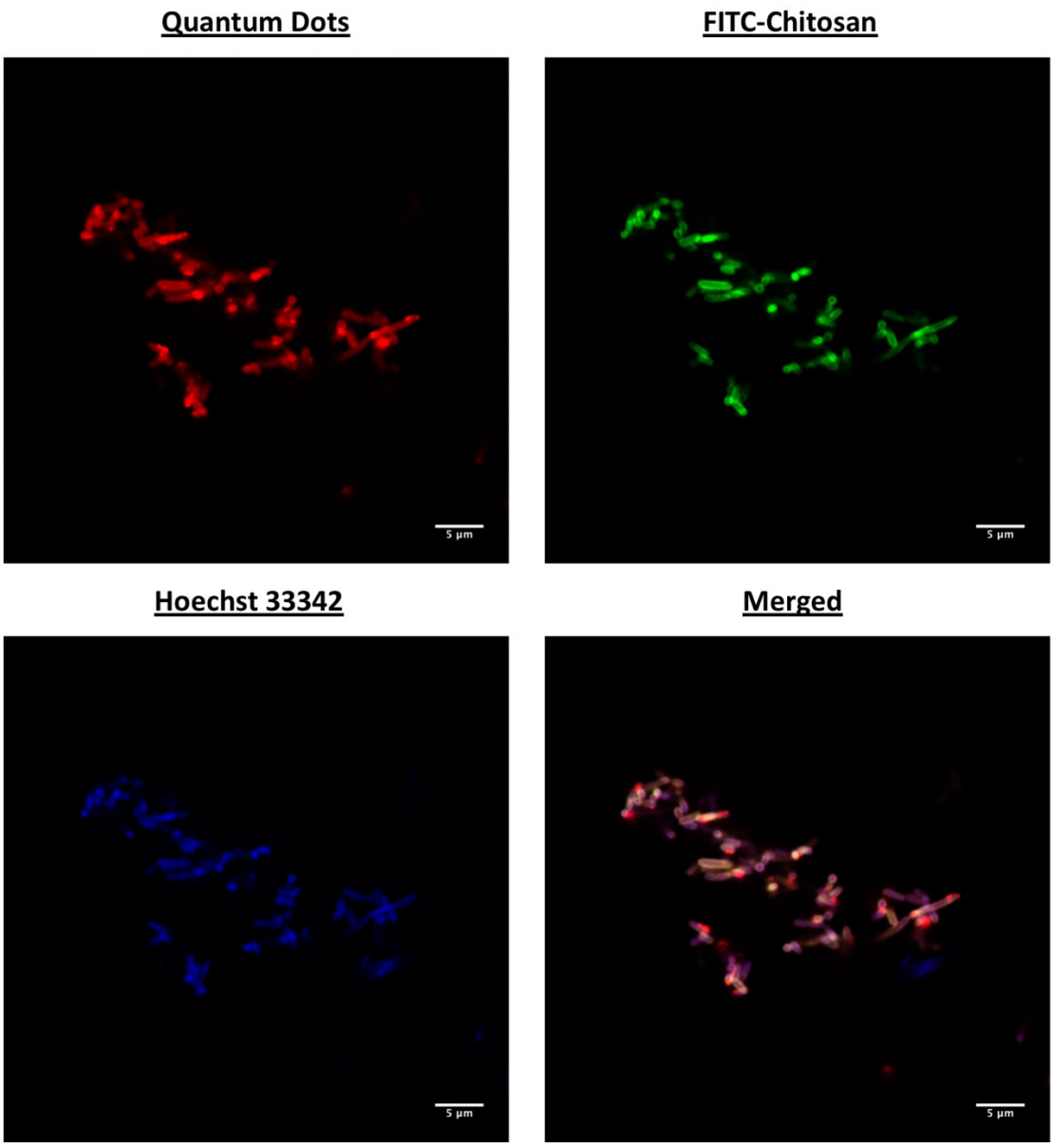

Figure 4.12: Confocal microscopy images of *E. coli* cells internally labeled with QD_{630nm} (red), coated with FITC-chitosan (green) and stained with Hoechst 33342 (blue).

TEM images were used to further confirm the internalization of quantum dots into the cells. As shown in Figure 4.13, the cells labeled with quantum dots have a darker intracellular space and increased contrast in comparison with non-labeled cells. This is a result of the heavy metal composition of the quantum dots, allowing for increased contrast when observed under TEM.

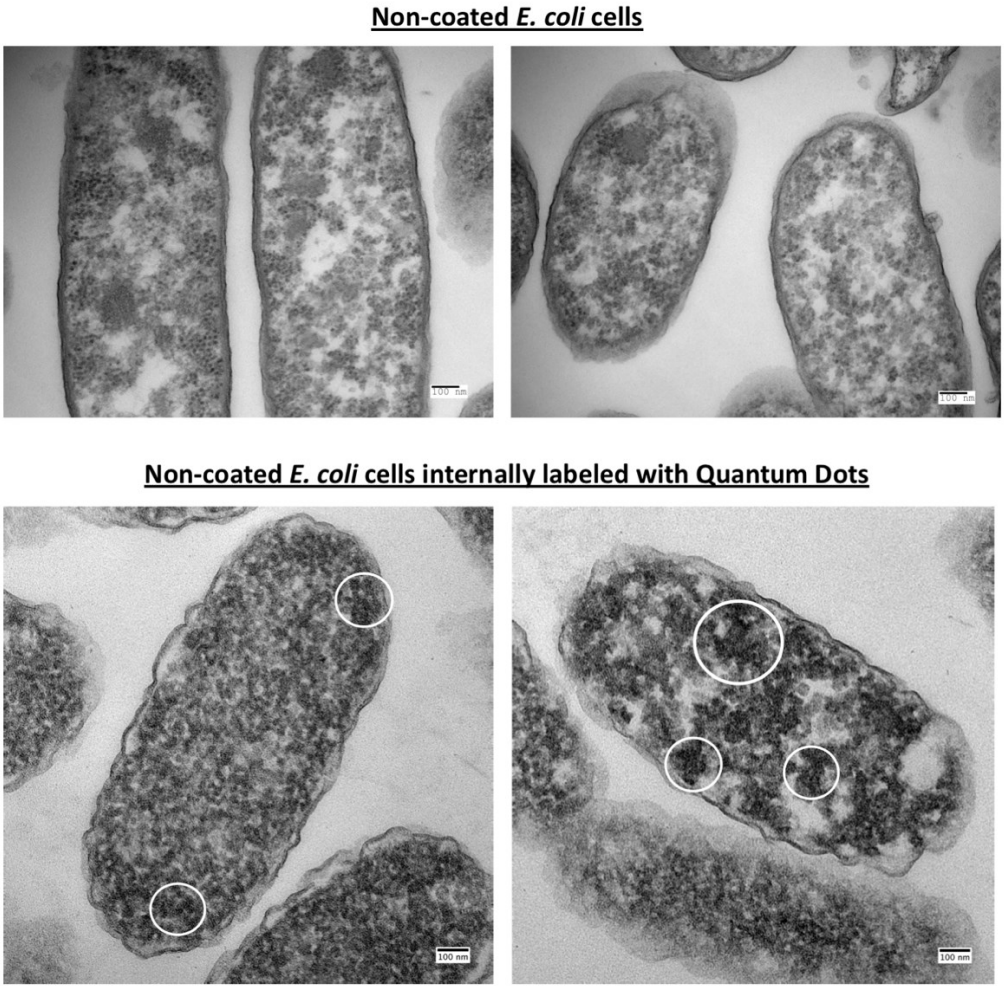

Figure 4.13: TEM images of non-coated *E. coli* cells (control) and non-coated cells incubated with quantum dots. White circles show example of areas with high contrast corresponding to the presence of quantum dots.

The QD-labeled cells were coated with eight layers of chitosan and alginate. The zeta potential of the QD-labeled non-coated cells show a decrease in magnitude from -54.67±1.1 mV for non-labeled *E. coli* to -32.7±1.0 mV after quantum dot labeling, which is likely associated with membrane disruption as a result of quantum dot internalization into the cells. Asides from that, the LbL coating showed very stable zeta potential values (>30 mV in magnitude) following a similar trend as the coating on live non-labeled cells discussed earlier (section 4.3).

Layer	Zeta Potential (mv)
L0	-32.7±1
L1 (CHI)	28.11±1.72
L2 (AL)	-36.08±2.79
L3 (CHI)	32±2.02
L4 (AL)	-32.25±1.37
L5 (CHI)	32.1±2.38
L6 (AL)	-30.02±1.65
L7 (CHI)	28.64±1.28
L8 (AL)	-32.65±1.17

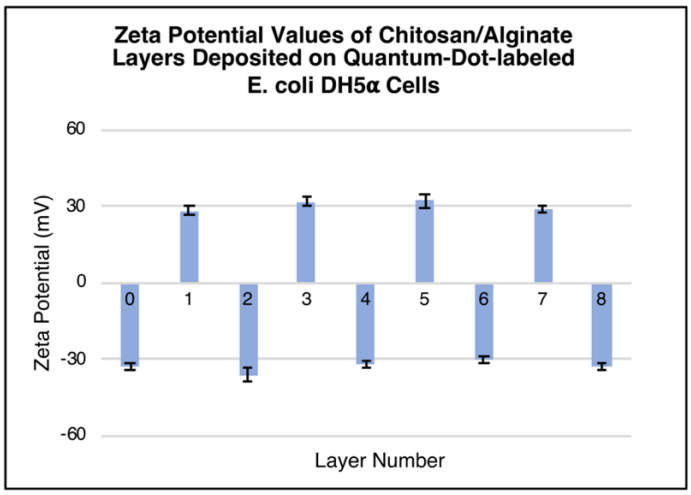

Figure 4.14: Zeta potential analysis of chitosan/alginate layer deposition onto *E. coli* cells labeled with QD_{630nm} in acetate buffer (10 mM, pH 5). The scale on the graph highlights the threshold for stability (±30 mV).

The coated cells carrying these quantum dots were also characterized using TEM (Figure 4.15) to study their morphology as well as identify any cell lysis that occurred when they were treated with the same detergent buffer used in section 4.4. The chitosan/alginate coating on these cells exhibited the same morphology and thickness as the results described earlier in section 4.3. Furthermore, the treatment with lysis buffer also provided with the same yield, although it was difficult to distinguish the presence of quantum dots in the empty vesicle.

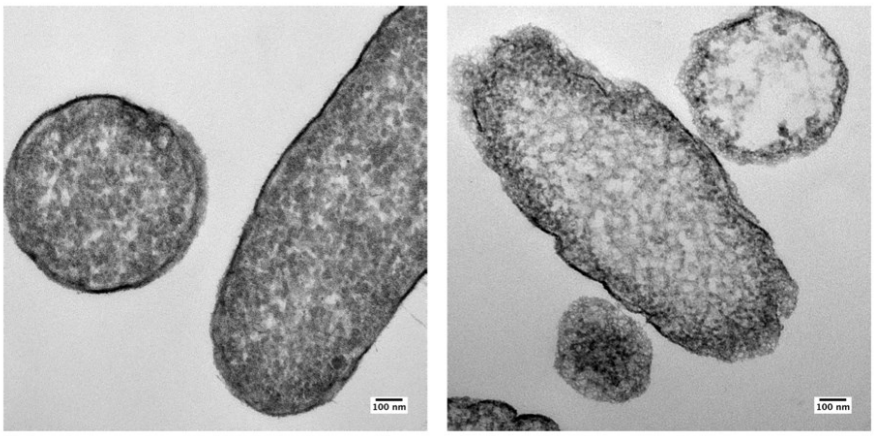

Figure 4.15: TEM images of quantum dot labeled cells coated with four bilayers of chitosan/alginate (left) and the same construct treated with lysis buffer (right)

5. DISCUSSION

The goal of the proposed study was to develop hollow capsules using chitosan and alginate while *E. coli* cells served as a sacrificial template. Experiments were designed to investigate the three main objectives outlined in the introduction section: encapsulate *E. coli* cells with alternating layers of chitosan and alginate; determine a suitable cell lysis protocol to form hollow microsphere; and encapsulate quantum dots into the cells as a cargo for the hollow microspheres. The results show the first objective was successfully achieved, while the second and third objectives showed promising results with some challenges. The implications of these results along with the challenges faced during the study are subsequently discussed in accordance with the correlated objective.

Objective 1: Encapsulation of *E. coli* DH5α cells with alternating layers of chitosan and alginate

The coating protocol was optimized using polystyrene microspheres as well as fixed *E. coli* cells before using live cells as templates. As mentioned in earlier chapters, this was done to minimize aggregation and ensure the production of stable and well-dispersed constructs. Aggregation is one of the main challenges involved in layer-by-layer self-assembly of polyelectrolytes. It occurs due to weakly charged polymers/substrates that do not have adequate repulsion between neighboring particles, which results in the conglomeration of the particles or substrates. Therefore, there must be high charge concentration on the polyelectrolytes as well as high concentration of the polyelectrolyte itself in order to achieve saturation during the adsorption process. This results in the adsorption of polyelectrolytes onto charged substrates with complete

coverage to cause repulsion between neighboring particles and stabilize the coated substrates in solution.

As mentioned in the introduction (section 2.4), the formation of layer-by-layer complexes is fast and governed by the displacement of counter ions adsorbed onto the polyelectrolytes that are forming such complex.[32] However, a mismatch in the molecular mass of the two electrolytes can result in most of the counter ions being displaced by the adsorption of several smaller polyelectrolytes onto the longer polymer with some of the counter ions remaining in their place. These counter ions shield a region in the polymer that is not compensated by the polyelectrolyte complex formation (Figure 5.1B) and this region is free to interact with other particles/polymers, thus opening the opportunity for aggregate formation. Therefore, achieving saturation during LbL coating requires balancing this stoichiometric difference to achieve saturation with the deposition of each layer. This can be calculated theoretically by taking into account the molecular weight of each polymer, the concentration of charged entities in each molecule and their degree of ionization at a given pH. These values can then be corroborated with experimental findings such as zeta potential measurements, QCM-D or other quantitative tools used to characterize LbL films.[34]

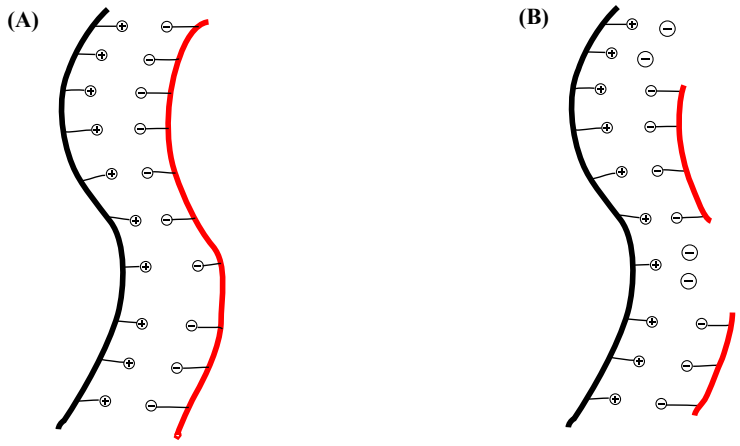

Figure 5.7: Illustrations of the interaction between oppositely charged polyelectrolytes with stoichiometrically balanced mixtures (A) and non-stoichiometric complexes (B).

In this project, the chitosan used for LbL assembly was ~300 kDa, whereas alginate was only ~150 kDa. Based on the Henderson-Hasselbalch equation, it is expected that ~97% of the amine groups on the chitosan to hold a positive charge and alginate is expected to have a similar percentage of deionized groups at pH 5 based on its pKa. Taking into account the 90% deacetylation of chitosan, this results in a theoretical stoichiometric ratio of 1.8:1 (alginate:chitosan) for polymer concentrations to achieve charge compensation. However, more chitosan was required during the coating process than alginate, which was determined experimentally using zeta potential measurements. This could be a result of steric hinderance by nearby acetyl groups on chitosan, which can have a shielding effect on free amine groups. Furthermore, the hydrophobic backbone of the polymer contributes to the reduction of ion-ion interaction via steric hinderance and reduced charge density.[33] As a result, chitosan can have a lower surface charge than what its deionization percentage predicted, leading to the requirement for adding more chitosan to achieve charge equilibrium during coating.

Despite the attempts to achieve adequate charge compensation, aggregations can still occur since both polyelectrolytes are considered weak polyelectrolytes. As shown in Figure 5.2, aggregation forms in a two-step mechanism for polyelectrolyte complexes. Initial aggregations due to a few regions without homogenous surface charge (or slight excess in titrants) forms smaller particles. These smaller particles can flocculate to become macroscopic aggregates if these aggregates are then met with an excess polyelectrolyte.[47] Therefore, coating protocols must proceed with the exact amount of polymer deposition on the surface of templates to avoid excess polymer in solution and potential flocculation. This is commonly achieved by a washing step to remove excess polyelectrolytes or using titration to calculate the exact amount needed for saturation. In this project, titration was used to determine the point of saturation and then a 50%

excess of the polyelectrolyte (by weight) was introduced to achieve complete coverage. The excess polyelectrolyte was then removed from the solution via washing with centrifugation.

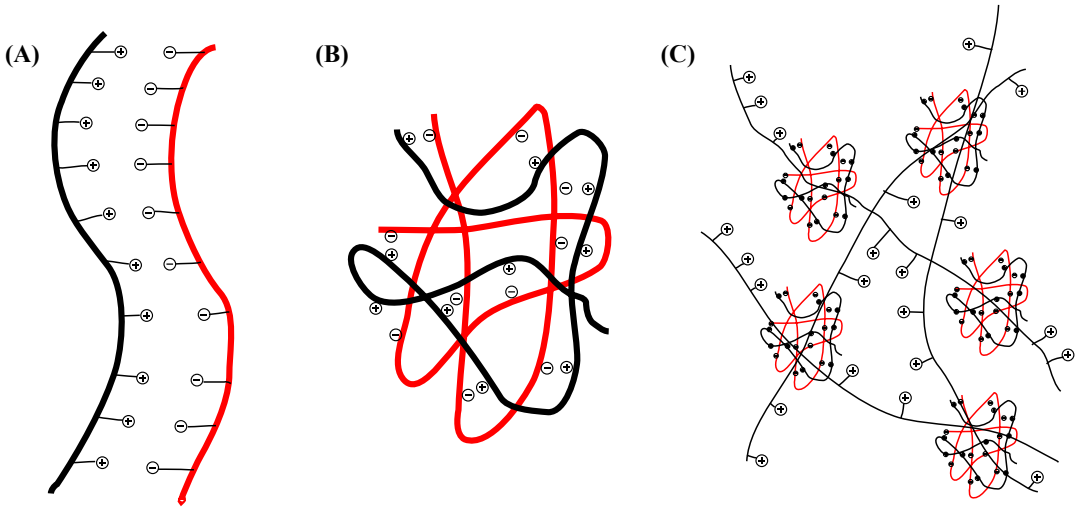

Figure 5.8: Illustration of the two-step aggregation formation model. A balanced interaction between oppositely charged polyelectrolytes(A) as well as the initial aggregation (B) and macroscopic flocculation (C) are shown.

In addition, the presence of aggregation in LbL assembled systems can be affected by ionic strength, which was examined in this study and the results were outlined in section 4.2. This is a particularly important factor when coating biological samples as a certain concentration of salt is necessary for the survival of cells. However, this can also be seen as detrimental to the formation of well-dispersed polyelectrolyte layers. As described in the introduction (section 2.4), intrinsic charge compensation in low salt concentration results in the highest amount of ionic interaction as its driven by entropy due to the displacement of counterions. On the other hand, increased concentration of counterions reduces the ionic interaction between layers due to the bulk extrinsic charge compensation.[12,39] Therefore, optimization of this factor is crucial to producing aggregate-free LbL constructs on biological samples while preserving the integrity of the template. In this project, it was determined through zeta-potential experiments that using a buffer without added

salts such as NaCl and KCl produced LbL constructs with the best stability and least amount of aggregation.

Furthermore, centrifuge speeds are also an important factor to consider in determining coating strategies. In regard to the use of weak electrolytes with soft templates such as cells, high centrifuge speed results in the irreversible flocculation of samples. Due to this reason, some studies have opted in using filtration or avoiding excess polymer via titration for more sensitive cell types that cannot tolerate the centrifuge speeds necessary to isolate them from the viscous polymer solutions.[6,47] Asides from the centrifuge speed, the type of flask used during centrifugation also affects how compact the pellet is and whether or not it will cause irreversible aggregation of the sample. Cone-shaped pellets experience much larger forces during centrifugation in comparison with flat-shaped pellets due to the increased height. As a result, using a flask or a tube with a round bottom, or having a swing-bucket centrifuge to ensure the LbL construct does not pellet in a cone or wedge-type geometry is important to reduce aggregation.[82] This was also verified in the current project by switching from a 15 mL Falcon tube, which has a narrower bottom, to a 50 mL Falcon tube, which allowed for a flatter and less compact pellet. In addition, this speaks to the versatility of the LbL system since alternative coating methods such as microfluidic setups are also available to accommodate force-sensitive substrates and achieve similar results.

Objective 2: Determination of a suitable cell lysis protocol to form hollow microspheres

The need for choosing a mild lysis protocol to break down and dissolve the *E. coli* cell structure and its macromolecular components while maintaining multilayer composition has been established in earlier chapters. Most protocols utilize detergents or physical methods such as freeze-drying to disrupt the outer membrane and use lysozyme to digest the peptidoglycan layer

of the membrane. Once this occurs, DNase or sonication can be used to break apart DNA and without the addition of protease inhibitors, the proteins inside the cells would also degrade as a consequence of the proteases released by the cells. Alternative protocols examined in this study include using alcohols such as ethanol and isopropyl alcohol (IPA), which lyse the cell via osmotic shock. Using saline above physiological concentrations can also disrupt the cells in a similar fashion and is often used in the literature but, it was avoided since high ionic strength in solution can lead to flocculation.[66–68] Heating the sample is also detrimental to the LbL construct even though it is a protocol often used to extract DNA from *E. coli*.[70] Out of all these methodologies, the one with the best result in terms of total breakdown of cell components was the detergent buffer. While alcohols caused cell death, they did not cause sufficient breakdown of the cell components. Therefore, the detergent-based protocol was chosen as the optimal protocol. The non-ionic detergent Triton-X was used to minimize disruption to the layers, and this was also evident in the results. Furthermore, the addition of 2 mM ethylenediaminetetraacetic acid (EDTA) as a chelator was important to disrupt outer membrane by binding and removing magnesium ions, which are critical to stabilizing the lipopolysaccharides in the outer membrane.

The lysis of non-coated cells was easily verified by the drastic reduction in turbidity and increase in viscosity of the sample due to the liberation of DNA into the solution. This was only observed with detergent-lysozyme based protocols and no other lysis reagent. However, measuring the level of degradation in lysates containing coated cells was a challenging task due to the small size of the multilayer construct and the lack of adequate resolution to distinguish between intact cells vs. hollow microshells with good efficiency using confocal microscopy. Therefore, accurate characterization could only be accomplished using TEM, which was a relatively lengthy process and difficult for quicker validation and tune up of experimental parameters.

Permeability seems to be one of the main issues with the lysis protocol. Even when the detergent-based protocol was effective in providing good quality lysate, the same result was not observed with coated cells treated in the same buffer. Layer-by-layer self-assembly has many applications in the literature including mediating the controlled release of substances as well as the encapsulation and shielding of substrates from outside environment. This level of versatility is the consequence of being able to control layer permeability. In this scenario, the multilayer membrane would have to effectively evacuate various macromolecules including DNA, proteins and detergent micelles containing membrane lipids. The results show a low yield in hollow microcapsules, which could be correlated with this issue in permeability. Furthermore, there have been theories indicating that layers constructed in low ionic concentrations contain few but large defects that can allow for exchange of materials but overall show a lower rate of permeation. On the other hand, multilayers constructed in high ionic concentrations have better permeability due to the formation of smaller and more abundant pores.[12]

Another reason for the low yield of hollow microcapsules could be instability of the microcapsules themselves. While these microcapsules are expected to be stable in solution, it has been shown in the literature that some hollow capsules, especially ones in the micron size range, tend to collapse and form flat structures once the core template has been removed. If capsule instability is an issue, it would imply that the observed yield in this study represents a much smaller subset of the actual yield of hollow microcapsules. Since they would have lost their integrity once the template was removed, they would not have been accounted for during characterization. Additional studies are required to confirm this and also investigate how the stability of such capsules can be improved.[61,62]

Although commonly established lysis protocols were chosen for this project, one factor that can play a part in the lysis of *E. coli* cells is chitosan itself. Chitosan is widely established as an antimicrobial and often used in products to limit the growth of bacteria, including *E. coli*. There is some evidence in the literature to support a positive correlation between chitosan MW and antibacterial activity, with a decrease in the former leading to an increase in the latter. Since the chitosan used in this study is high MW (~300 kDa), it can be assumed that this would have a low potency towards bacterial cell destruction. However, there is also evidence in the literature against this with studies that demonstrate how an increase in chitosan MW leads to an increase in antimicrobial activity.[74,81] Overall, it is evident that there are several aspects in the lysis protocol that could be reason for the observed low yield of microcapsules and addressing such factors must be a particular area of focus in future directions of such study.

Objective 3: Encapsulation of quantum dots into cells before LbL coating as a cargo for the subsequent hollow vesicles

Quantum dots were selected as a preferred cargo for the hollow microshells in this project due to their photo and thermostability, long shelf life as well as ease of tracking via microscope. While small drug molecules are able to diffuse into the bacteria cell with ease, quantum dot uptake in bacteria occurs in a similar fashion as the uptake of small plasmids and therefore require competent cells. These are bacteria cells with compromised membranes due to the presence of divalent ions such as Ca^{2+} and as a result, they allow for the internalization of large macromolecules and nanoparticles.[71] In this project, the quantum dots were dispersed in 2% Triton-X detergent and then added to the cell culture in buffer to incubate for one hour. As mentioned earlier, Triton-X detergent is often used to compromise the integrity of the *E. coli* outer

membrane in lysis protocols. Therefore, the presence of a detergent not only help solubilizing the quantum dots, but it also diffuses better within the hydrophobic membrane. However, this could also cause disruption of the membrane-bound proteins and reduce the surface charge of the cells, which was a phenomenon that was observed in the zeta-potential measurements of QD-labeled cells (section 4.6).

The uptake of quantum dots into the cells was also characterized via confocal microscopy. QDs with an emission wavelength of 630 nm were used in this project as their emission wavelength does not overlap with that of both Hoechst 33342 and FITC-chitosan fluorophores. Therefore, it allows for the co-localization of quantum dots and DNA inside the *E. coli* by labeling with Hoechst as a DNA-tagging fluorophore in QD-labeled cells. FITC-chitosan allows to confirm successful layer deposition onto the cells. The narrow emission wavelength of QDs make them ideal for immunostaining experiments and the results obtained in this study support this phenomenon.

Additionally, TEM experiments showed increased intracellular contrast in the presence of quantum dots when compared to control cells with no quantum dots. QD-labeled cells coated with four bilayers of chitosan/alginate were also treated with lysis buffer and showed very low yield of hollow vesicles in a similar fashion to the other lysis experiments. It was also difficult to distinguish the quantum dots in the hollow vesicle during TEM experiments, which could have been caused by the release of quantum dots during the lysis procedure. Further studies are required to evaluate this outcome with different size quantum dots as well as assess the release profile of the QDs from the microcapsules and evaluate the potential of such microcapsules as delivery systems for therapeutics.

6. CONCLUSION AND FUTURE DIRECTIONS

The proposed study evaluated the development of hollow microspheres through layer-by-layer self-assembly of chitosan and alginate while using *E. coli* as a sacrificial core template. The results illustrate that robust and stable chitosan/alginate nanofilms can be formed onto *E. coli* cells with nanometric thickness. Polystyrene microspheres as well as fixed *E. coli* cells were used to determine optimal coating conditions for the formation of these nanofilms. Several lysis protocols were tested for the production of hollow microshells from this construct by using mild cell lysis conditions. Some hollow capsules were observed under TEM with good stability and increased film thickness in comparison to capsules with intact *E. coli* cells in their core. Furthermore, quantum dots were used to test the efficacy of this system and it was shown that LbL coated cells can be successfully synthesized onto *E. coli* cells that are internally labeled with quantum dots. Additional studies are required to increase the yield of hollow microcapsules from the lysis protocol as well as testing the release profile of the QDs, which serve as a proof-of-concept cargo for the capsules.

In future studies, several aspects of the project can be further addressed. Increasing the permeability of the capsules is an important factor in increasing the yield of the lysis protocol and one way this can be achieved is by using higher ionic strength during coating. While the chitosan/alginate complex used in this project did not form stable films at higher ionic strength, other polymer systems such as poly-L-lysine can be investigated to address this concern. In addition, self-crosslinking bilayers can be implemented to ensure the stability of LbL films that are produced at a higher ionic strength. This would allow for increased porosity while maintaining

the integrity of the film and improving the permeability of the capsule. One example of such systems is mentioned in the study done by Knopf-Marques et al. where modified hyaluronic acid with free aldehyde groups were used as a cross-linking site for layer-by-layer coating applications.[72] This resulted in the formation of imine bonds between the layers due to the free aldehyde group reacting with amine groups, which are often present in polycations such as poly-L-lysine or polyallylamine. Other studies have explored the use of Staudinger ligation chemistry between azide and carbonyl groups to produce an amide linkage in the presence of phenylphosphine.[83] Grafting each reactive group onto the polycation/polyanion provides crosslinking in layer-by-layer coatings after self-assembly of the polymer layers. Overall, increase in permeability of the multilayer construct is necessary for better yield in lysis and improving the stability of such system via crosslinking might be a necessary approach to achieve it.

Additionally, centrifugation can be replaced with other techniques such as filtration for separation of coated substrates to avoid aggregation while improving layer permeability in high ionic strength solution. Several studies have shown the efficacy of a filtration step in the coating of sensitive substrates such as red blood cells[6] or pancreatic islets[84]. Removing excess polyelectrolyte via filtration exerts significantly less forces on the coating as well as the substrates and therefore, it could be useful towards developing the coating described in the project at a high ionic strength. Coating via microfluidic setups can also be exploited in future experiments and several designs have been published in the literature towards LbL applications.[85,86] Since the substrate can be precisely manipulated within microfluidic channels while polyelectrolyte or buffer solutions are flowed through the channel, it is also more favourable than centrifugation for force-sensitive constructs and greatly accelerates layer deposition process overall. While centrifugation might be the easiest and ,in often cases, cheapest solution towards purification of coated substrates

from excess polyelectrolyte, the other proposed solutions could be more effective in producing high yield and high quality coated constructs.

Different strains of bacteria can also be exploited for lysis efficiency, especially those that can contain bacteriophages or other internal mechanisms for cell disintegration. Incorporation of genetic material that can allow for self-induced cell death after coating can allow for an easier method of dissolving the core. This would require less components for lysis such as detergent and enzymes, which add to the amount of substance that has to travel through the pores of the nanofilm. Lysozyme is 14.3kDa (Sigma) while DNAse can be upwards of 40kDa (Invitrogen) and the micelle MW of Triton-X can be 90kDa[87]. These are all very large molecules in this context and the transport of such substances across the nanolayers to break down and release cellular content can increase the burden on the pores inside the nanolayers. As a result, avoiding such burden by the use of self-destructing bacteria can allow for an increased clearance of materials from the core of the construct to provide a higher yield of microcapsules. While this might require more initial work, an established system would become much efficient since it would require less time and effort for lysis and isolation of hollow capsules as a whole.[88]

Furthermore, different size QDs can be tested to evaluate the influence of particle/molecule size on the retention of cargo during the production of hollow microshells. QD release can be measured by a variety of fluorescence studies including confocal microscopy and fluorescence spectrometry. Quantitative analysis of the retention/release of QDs is important to firmly establish the proof-of-concept that such microcapsule can be used towards cargo delivery applications in therapeutics as well as imaging. Further characterization of the construct can also be done using elemental analysis (EDX) on SEM, which can also help to measure the pore size on these

multilayer films. This can be important in future studies for further establishing the relationship between high ionic strength and high permeability, which could be a result of increased pore size or pore distribution. In conclusion, the hollow microcapsules described in this project hold the potential as a biomaterial for systemic controlled delivery of therapeutics and imaging probes. The novel protocol used for the synthesis of these microcapsules further expands the potential of such technique with the ability to use not only *E. coli* but other cell types as potential templates for future investigation.

7. REFERENCES

1. Neu, B. *et al.* Biological cell as templates for hollow microcapsules. *J. Microencapsul.* **18**, 385–395 (2001).
2. Ribeiro, C. *et al.* Preparation of well-dispersed chitosan/alginate hollow multilayered microcapsules for enhanced cellular internalization. *Molecules* **23**, (2018).
3. Xie, Y. L., Wang, M. J. & Yao, S. J. Preparation and characterization of biocompatible microcapsules of sodium cellulose sulfate/chitosan by means of layer-by-layer self-assembly. *Langmuir* **25**, 8999–9005 (2009).
4. Richardson, J. J., Björnmalm, M. & Caruso, F. Technology-driven layer-by-layer assembly of nanofilms. *Science (80-.).* **348**, 411 (2015).
5. Chai, F. *et al.* Doxorubicin-loaded poly (Lactic-co-glycolic acid) nanoparticles coated with chitosan/alginate by layer by layer technology for antitumor applications. *Int. J. Nanomedicine* **12**, 1791–1802 (2017).
6. Mansouri, S., Merhi, Y., Winnik, F. M. & Tabrizian, M. Investigation of Layer-by-Layer Assembly of Polyelectrolytes on Fully Functional Human Red Blood Cells in Suspension for Attenuated Immune Response. *Biomacromolecules* **12**, 585–592 (2011).
7. Hillberg, A. L. & Tabrizian, M. Biorecognition through layer-by-layer polyelectrolyte assembly: In-situ hybridization on living cells. *Biomacromolecules* **7**, 2742–2750 (2006).
8. Patra, J. K. *et al.* Nano based drug delivery systems: recent developments and future prospects. *J Nanobiotechnol* **16**, 71 (2018).
9. Cortez, C. *et al.* Targeting and uptake of multilayered particles to colorectal cancer cells. *Adv. Mater.* **18**, 1998–2003 (2006).
10. Xu, S., Olenyuk, B. Z., Okamoto, C. T. & Hamm-Alvarez, S. F. Targeting receptor-mediated endocytotic pathways with nanoparticles: Rationale and advances. *Adv. Drug Deliv. Rev.* **65**, 121–138 (2013).
11. Yameen, B. *et al.* Insight into nanoparticle cellular uptake and intracellular targeting. *J. Control. Release* **190**, 485–499 (2014).
12. Mansouri, S., Winnik, F. M. & Tabrizian, M. Modulating the release kinetics through the control of the permeability of the layer-by-layer assembly: a review. *Expert Opin. Drug Deliv.* **6**, 585–597 (2009).

13. Freiberg, S. & Zhu, X. X. Polymer microspheres for controlled drug release. *Int. J. Pharm.* **282**, 1–18 (2004).
14. Shi, J., Du, C., Shi, J., Wang, Y. & Cao, S. Hollow Multilayer Microcapsules for pH-/Thermally Responsive Drug Delivery using Aliphatic Poly(urethane-amine) as Smart Component. *Macromol. Biosci.* **13**, 494–502 (2013).
15. Zhang, Y., Chen, C., Wang, J. & Zhang, L. Polysaccharide-based polyelectrolytes hollow microcapsules constructed by layer-by-layer technique. *Carbohydr. Polym.* **96**, 528–535 (2013).
16. Wang, A. J., Lu, Y. P. & Sun, R. X. Recent progress on the fabrication of hollow microspheres. *Mater. Sci. Eng. A* **460–461**, 1–6 (2007).
17. Keeney, M. *et al.* Nanocoating for biomolecule delivery using layer-by-layer self-assembly. *J Mater Chem B Mater Biol Med* **3**, 8757–8770 (2016).
18. Liu, P. Stabilization of layer-by-layer engineered multilayered hollow microspheres. *Adv. Colloid Interface Sci.* **207**, 178–188 (2014).
19. Ghosh, S. K. *Functional Coatings*. (Wiley-VCH Verlag GmbH & Co. KGaA, 2006). doi:10.1002/3527608478
20. Zhang, S., Xing, M. & Li, B. Biomimetic layer-by-layer self-assembly of nanofilms, nanocoatings, and 3D scaffolds for tissue engineering. *Int. J. Mol. Sci.* **19**, (2018).
21. Blodgett, K. B. Films Built by Depositing Successive Monomolecular Layers on a Solid Surface. *J. Am. Chem. Soc.* **57**, 1007–1022 (1935).
22. Decher, G. & Schlenoff, J. B. *Multilayer Thin Films: Sequential Assembly of Nanocomposite Materials: Second Edition* **1–2**, (Wiley-VCH Verlag GmbH & Co. KGaA, 2012).
23. Fujimori, A. Langmuir-Blodgett (LB) Film. in *Encyclopedia of Polymeric Nanomaterials* 1044–1050 (Springer Berlin Heidelberg, 2015). doi:10.1007/978-3-642-29648-2_145
24. Matovic, J. & Jakšić, Z. Nanomembrane: A New MEMS/NEMS Building Block. *Micro Electron. Mech. Syst.* (2009).
25. Kurihara, K. Self-Assembled Monolayer. *Encycl. Polym. Nanomater.* 1–3 (2015). doi:10.1007/978-3-642-36199-9_157-1
26. Sagiv, J. Organized Monolayers by Adsorption. 1. Formation and Structure of Oleophobic Mixed Monolayers on Solid Surfaces. *J. Am. Chem. Soc.* **102**, 92–98 (1980).

27. Tsai, P. S., Yang, Y. M. & Lee, Y. L. Fabrication of hydrophobic surfaces by coupling of Langmuir-Blodgett deposition and a self-assembled monolayer. *Langmuir* **22**, 5660–5665 (2006).
28. Netzer, L., Iscovici, R. & Sagiv, J. Adsorbed monolayers versus Langmuir-Blodgett monolayers - why and how? I: From monolayer to multilayer, by adsorption. *Thin Solid Films* **99**, (1982).
29. Iler, R. K. Multilayers of colloidal particles*. *J. Colloid Interface Sci.* **21**, (1966).
30. Decher, G. & Schmitt, J. Fine-Tuning of the film thickness of ultrathin multilayer films composed of consecutively alternating layers of anionic and cationic polyelectrolytes. in *Trends in Colloid and Interface Science VI* **89**, 160–164 (1992).
31. Decher, G. Fuzzy nanoassemblies: Toward layered polymeric multicomposites. *Science (80-.).* **277**, 1232–1237 (1997).
32. Guzmán, E., Mateos-Maroto, A., Ruano, M., Ortega, F. & Rubio, R. G. Layer-by-Layer polyelectrolyte assemblies for encapsulation and release of active compounds. *Adv. Colloid Interface Sci.* **249**, 290–307 (2017).
33. Bertrand, P., Jonas, A., Laschewsky, A. & Legras, R. Ultrathin polymer coatings by complexation of polyelectrolytes at interfaces: suitable materials, structure and properties. *Macromol. Rapid Commun* **21**, (2000).
34. Koetz, J. & Kosmella, S. *Polyelectrolytes and Nanoparticles*. (2007). doi:10.1007/978-3-540-46382-5
35. Yan, Y., Björnmalm, M. & Caruso, F. Assembly of layer-by-layer particles and their interactions with biological systems. *Chem. Mater.* **26**, 452–460 (2014).
36. Sato, K., Yoshida, K., Takahashi, S. & Anzai, J. ichi. pH- and sugar-sensitive layer-by-layer films and microcapsules for drug delivery. *Adv. Drug Deliv. Rev.* **63**, 809–821 (2011).
37. Berg, J. M., Tymoczko, J. L. & Stryer, L. *Biochemistry*. (W.H. Freeman, 2012).
38. Richardson, J. J. *et al.* Innovation in Layer-by-Layer Assembly. *Chem. Rev.* **116**, 14828–14867 (2016).
39. P.M., V., Bayraktar, O. & Pico, G. A. *Polyelectrolytes*. *Engineering Materials* (Springer International Publishing, 2014). doi:10.1007/978-3-319-01680-1
40. Yan, Y., Such, G. K., Johnston, A. P. R., Lomas, H. & Caruso, F. Toward therapeutic delivery with layer-by-layer engineered particles. *ACS Nano* **5**, 4252–4257 (2011).

41. Elizarova, I. S. & Luckham, P. F. Fabrication of polyelectrolyte multilayered nano-capsules using a continuous layer-by-layer approach. *J. Colloid Interface Sci.* **470**, 92–99 (2016).
42. Jiang, C. *et al.* Mechanical Properties of Robust Ultrathin Silk Fibroin Films. *Adv. Funct. Mater.* **17**, 2229–2237 (2007).
43. Wang, J., Chao, Y., Wan, Q., Zhu, Z. & Yu, H. Fluoridated hydroxyapatite coatings on titanium obtained by electrochemical deposition. *Acta Biomater.* **5**, 1798–1807 (2009).
44. Caruso, F., Niikura, K., Furlong, D. N. & Okahata, Y. 1. Ultrathin Multilayer Polyelectrolyte Films on Gold: Construction and Thickness Determination. *Langmuir* **13**, 3422–3426 (2002).
45. Stevenson, K., McVey, A. F., Clark, I. B. N., Swain, P. S. & Pilizota, T. General calibration of microbial growth in microplate readers. *Sci. Rep.* **6**, 38828 (2016).
46. Guzmán, E. *et al.* 3D solid supported inter-polyelectrolyte complexes obtained by the alternate deposition of poly(diallyldimethylammonium chloride) and poly(sodium 4-styrenesulfonate). *Beilstein J. Nanotechnol.* **7**, 197–208 (2016).
47. Nayef, L., Castiello, R. & Tabrizian, M. Washless Method Enables Multilayer Coating of an Aggregation-Prone Nanoparticulate Drug Delivery System with Enhanced Yields, Colloidal Stability, and Scalability. *Macromol. Biosci.* **17**, 1600535 (2017).
48. Kujawa, P., Moraille, P., Sanchez, J., Badia, A. & Winnik, F. M. Effect of molecular weight on the exponential growth and morphology of hyaluronan/chitosan multilayers: A surface plasmon resonance spectroscopy and atomic force microscopy investigation. *J. Am. Chem. Soc.* **127**, 9224–9234 (2005).
49. Ferreira, D. C. M., Mendes, R. K. & Kubota, L. T. Kinetic studies of HRP adsorption on ds-DNA immobilized on gold electrode surface by EIS and SPR. *J. Braz. Chem. Soc.* **21**, 1648–1655 (2010).
50. Lee, H. *et al.* Substrate-independent layer-by-layer assembly by using mussel-adhesive-inspired polymers. *Adv. Mater.* **20**, 1619–1623 (2008).
51. Gabor, F. 'Characterization of Nanoparticles Intended for Drug Delivery'. *Sci. Pharm.* **79**, 701–702 (2011).
52. Yoshida, K. *et al.* pH-Dependent Release of Insulin from Layer-by-Layer-Deposited Polyelectrolyte Microcapsules. *Polymers (Basel).* **7**, 1269–1278 (2015).

53. Lundin, M., Solaqa, F., Thormann, E., MacAkova, L. & Blomberg, E. Layer-by-layer assemblies of chitosan and heparin: Effect of solution ionic strength and pH. *Langmuir* **27**, 7537–7548 (2011).

54. Berth, G., Voigt, A., Dautzenberg, H., Donath, E. & Möhwald, H. Polyelectrolyte complexes and layer-by-layer capsules from chitosan/chitosan sulfate. *Biomacromolecules* **3**, 579–590 (2002).

55. Lutkenhaus, J. L., Hrabak, K. D., McEnnis, K. & Hammond, P. T. Elastomeric flexible free-standing hydrogen-bonded nanoscale assemblies. *J. Am. Chem. Soc.* **127**, 17228–17234 (2005).

56. Jaber, J. A. & Schlenoff, J. B. Dynamic viscoelasticity in polyelectrolyte multilayers: Nanodamping. *Chem. Mater.* **18**, 5768–5773 (2006).

57. Mansouri, S. *et al.* Silencing red blood cell recognition toward anti-a antibody by means of polyelectrolyte layer-by-layer assembly in a two-dimensional model system. *Langmuir* **25**, 14071–14078 (2009).

58. Thierry, B., Winnik, F. M., Merhi, Y., Silver, J. & Tabrizian, M. Bioactive coatings of endovascular stents based on polyelectrolyte multilayers. *Biomacromolecules* **4**, 1564–1571 (2003).

59. Macdonald, M. L. *et al.* Tissue integration of growth factor-eluting layer-by-layer polyelectrolyte multilayer coated implants. *Biomaterials* **32**, 1446–1453 (2011).

60. Lederer, F. L., Günther, T. J., Weinert, U., Raff, J. & Pollmann, K. Development of functionalised polyelectrolyte capsules using filamentous Escherichia coli cells. *Microb. Cell Fact.* **11**, 163 (2012).

61. Irigoyen, J. *et al.* Fabrication of hybrid graphene oxide/polyelectrolyte capsules by means of layer-by-layer assembly on erythrocyte cell templates. *Beilstein J. Nanotechnol.* **6**, 2310–2318 (2015).

62. Bhadra, D., Gupta, G., Bhadra, S., Umamaheshwari, R. B. & Jain, N. K. Multicomposite ultrathin capsules for sustained ocular delivery of ciprofloxacin hydrochloride. *J. Pharm. Pharm. Sci.* **7**, 241–251 (2004).

63. Baker, S., Griffiths, C. & Nicklin, J. *Microbiology: 4th Edition*. (2011).

64. Huang, W. *et al.* Employing Escherichia coli-derived outer membrane vesicles as an antigen delivery platform elicits protective immunity against Acinetobacter baumannii infection. *Sci. Rep.* **6**, 37242 (2016).
65. Humann, J. & Lenz, L. L. Bacterial peptidoglycan degrading enzymes and their impact on host muropeptide detection. *J. Innate Immun.* **1**, 88–97 (2009).
66. Nikaido, H. & Varra, M. Molecular Basis of Bacterial Outer Membrane Permeability Revisited. *Microbiol. Mol. Biol. Rev.* **49**, 1–32 (1985).
67. KOHN, A. Lysis of frozen and thawed cells of Escherichia coli by lysozyme and their conversion into spheroplasts. *J. Bacteriol.* **79**, 697–706 (1960).
68. Ingram, L. O. Mechanism of lysis of Escherichia coli by ethanol and other chaotropic agents. *J. Bacteriol.* **146**, 331–336 (1981).
69. Davies, R. C., Neuberger, A. & Wilson, B. M. The dependence of lysozyme activity on pH and ionic strength. *BBA - Enzymol.* **178**, 294–305 (1969).
70. Tsuchido, T., Katsui, N., Takeuchi, A., Takano, M. & Shibasaki, I. Destruction of the Outer Membrane Permeability Barrier of Escherichia coli by Heat Treatment. *Appl. Environ. Microbiol.* **50**, (1985).
71. Li, W. *et al.* Exploring the mechanism of competence development in Escherichia coli using quantum dots as fluorescent probes. *J. Biochem. Biophys. Methods* (2004).
72. Knopf-Marques, H. *et al.* Immunomodulation with Self-Crosslinked Polyelectrolyte Multilayer-Based Coatings. *Biomacromolecules* **17**, 2189–2198 (2016).
73. Yuan, Y., Chesnutt, B. M., Haggard, W. O. & Bumgardner, J. D. Deacetylation of chitosan: Material characterization and in vitro evaluation via albumin adsorption and pre-osteoblastic cell cultures. *Materials (Basel).* **4**, 1399–1416 (2011).
74. Jung, J., Cavender, G. & Zhao, Y. The contribution of acidulant to the antibacterial activity of acid soluble α- And β-chitosan solutions and their films. *Appl. Microbiol. Biotechnol.* **98**, 425–435 (2014).
75. Gomez, C. G., Rinaudo, M. & Villar, M. A. Oxidation of sodium alginate and characterization of the oxidized derivatives. *Carbohydr. Polym.* **67**, 296–304 (2007).
76. Ye, S., Wang, C., Liu, X. & Tong, Z. Multilayer nanocapsules of polysaccharide chitosan and alginate through layer-by-layer assembly directly on PS nanoparticles for release. *J. Biomater. Sci. Polymer Edn* **16,** 909-923 (2017).

77. Kumari, A. & Singh, R. R. Cytotoxicity testing of bare CdSe quantum dots and their encapsulated structure. in *AIP Conference Proceedings* **1860**, 20004 (2017).
78. Hirschey, M. D., Han, Y. J., Stucky, G. D. & Butler, A. Imaging Escherichia coli using functionalized core/shell CdSe/CdS quantum dots. *J. Biol. Inorg. Chem.* **11**, 663–669 (2006).
79. Ma, O. *et al.* Precise derivatization of structurally distinct chitosans with rhodamine B isothiocyanate. *Carbohydr. Polym.* **72**, 616–624 (2008).
80. Wu, E. L. *et al.* E. coli outer membrane and interactions with OmpLA. *Biophys. J.* **106**, 2493–2502 (2014).
81. Kim, K. W., Thomas, R. L., Lee, C. & Park, H. J. Antimicrobial Activity of Native Chitosan, Degraded Chitosan, and O-Carboxymethylated Chitosan. *J. Food Prot.* **66**, (2003).
82. Peterson, B. W., Sharma, P. K., van der Mei, H. C. & Busscher, H. J. Bacterial cell surface damage due to centrifugal compaction. *Appl. Environ. Microbiol.* **78**, 120–5 (2012).
83. Gattás-Asfura, K. M., Valdes, M., Celik, E. & Stabler, C. L. Covalent layer-by-layer assembly of hyperbranched polymers on alginate microcapsules to impart stability and permselectivity. *J. Mater. Chem. B* **2**, 8208–8219 (2014).
84. Wilson, J. T. *et al.* Cell surface engineering with polyelectrolyte multilayer thin films. *J. Am. Chem. Soc.* **133**, 7054–7064 (2011).
85. Priest, C. *et al.* Microfluidic polymer multilayer adsorption on liquid crystal droplets for microcapsule synthesis. *Lab Chip* **8**, 2182–2187 (2008).
86. Kantak, C., Beyer, S., Yobas, L., Bansal, T. & Trau, D. A 'microfluidic pinball' for on-chip generation of Layer-by-Layer polyelectrolyte microcapsules. *Lab Chip* **11**, 1030–1035 (2011).
87. Baker, M. R., Fan, G. & Serysheva, I. I. Single-particle cryo-EM of the ryanodine receptor channel. *Eur. J. Transl. Myol. - Basic Appl. Myol.* **25,** 35-48 (2015).
88. Pasotti, L., Zucca, S., Lupotto, M., Cusella De Angelis, M. G. & Magni, P. Characterization of a synthetic bacterial self-destruction device for programmed cell death and for recombinant proteins release. *J. Biol. Eng.* **5**, 8 (2011).